ORGANIC PROCESS RESEARCH & DEVELOPMENT
OPR&D

pubs.acs.org/OPRD

Review

Quest for a Cure: Potential Small-Molecule Treatments for COVID-19, Part 2

David L. Hughes*

Cite This: https://doi.org/10.1021/acs.oprd.1c00100

Read Online

ACCESS | Metrics & More | Article Recommendations

ABSTRACT: During the first year of the outbreak of the COVID-19 pandemic, many drugs and drug candidates have been evaluated as treatment options. None yet has proved to be an effective cure, but progress in controlling the disease has been made. In June 2020 we published an article that described the mechanistic rationale behind the repurposing of seven licensed drugs in clinical trials for the treatment of COVID-19 and reviewed synthetic routes to these drugs. Several developments have occurred since then. Remdesivir (trade name Veklury) has been approved for use in the U.S. and Europe. Dexamethasone, a steroid drug first approved in 1959, has shown mortality reduction in severe COVID patients. Molnupiravir, a new and promising oral antiviral drug, is being studied in late-stage clinical trials. In this review, we update synthetic work that has been recently published on remdesivir, provide an overview of several routes to molnupiravir, and review classical routes to dexamethasone as well as some of those more recently developed.

KEYWORDS: *remdesivir, molnupiravir, dexamethasone, COVID-19, repurpose*

An analysis of 1988 clinical studies in progress in June 2020 revealed that 172 drugs or investigational drug candidates were being investigated for the treatment and/or prevention of SARS CoV-2.[1] Many of these are licensed drugs that are approved for other indications and are being repurposed for the treatment of SARS CoV-2. Some of these drugs have demonstrated partial efficacy, many have shown no efficacy, and many are still progressing through clinical trials. One positive trend over the first year of the virus is that mortality rates have decreased, as shown in Figure 1 for the world, the United States, and Europe, although the rates have leveled off at about 2% during the first 3 months of 2021.[2] While the metric of deaths per capita is an imprecise measure that does not account for many demographic factors, it does show that overall progress is being made in the treatment of COVID-19. While much of this may be attributable to an overall better understanding of how to treat the disease, it is quite possible that several of the drugs under study and now in routine use are contributing to the improvement in outcomes. It is also possible that some of the early experimental treatments may have done more harm than good.[2]

In June 2020 we published an article that described the mechanistic rationale behind the repurposing of seven licensed drugs in clinical trials for the treatment of COVID-19 and reviewed synthetic routes to these drugs, including remdesivir, hydroxychloroquine, favipiravir, pirfenidone, baricitinib, camostat, and lopinavir/ritonavir.[3] Several developments have occurred since then. Remdesivir (trade name Veklury) has been approved for use in the U.S. and Europe. Dexamethasone, a steroid drug first approved in 1959, has shown mortality reduction in severe COVID patients. Molnupiravir, a new and promising oral antiviral drug, is being studied in late-stage clinical trials. In this review, we update synthetic work that has been recently published on remdesivir (**1**), provide an overview of several routes to molnupiravir (**2**), and review classical routes to dexamethasone (**3**) as well as some of those more recently developed. The structures of **1**−**3** are shown in Chart 1.

1. REMDESIVIR (VEKLURY)

On October 22, 2020, the U.S. Food and Drug Administration (FDA) approved the antiviral drug Veklury (remdesivir) for use in adults and pediatric patients (12 years of age and older and weighing at least 40 kg) for the treatment of COVID-19 requiring hospitalization. The approval followed an Emergency Use Authorization granted on May 1, 2020. The approval was based on demonstration of a decreased time to recovery in patients hospitalized for severe COVID-19, irrespective of disease severity.[4]

On July 3, 2020, the European Commission granted conditional marketing authorization for Veklury for the treatment of COVID-19 in adults and adolescents (12 years of age and older and weighing at least 40 kg), with pneumonia requiring supplemental oxygen.[5]

1.1. Update on Remdesivir Clinical Trials. Three well-controlled clinical trials involving remdesivir for the treatment of COVID-19 have read out over the past year, including the Adaptive COVID-19 Treatment Trial (ACTT-1), the SOLIDARITY trial, and a trial in moderately ill patients.

Received: March 23, 2021

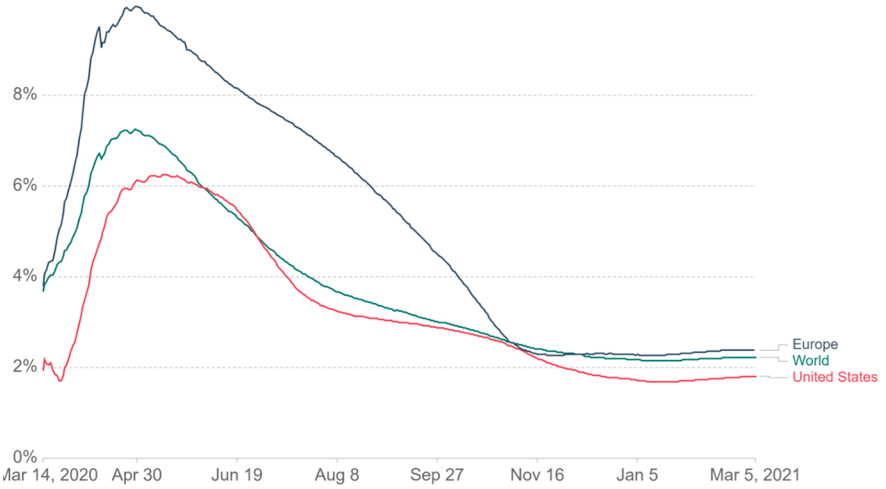

Figure 1. Death rates from COVID-19.

Chart 1. Structures of Remdesivir, Molnupiravir, and Dexamethasone

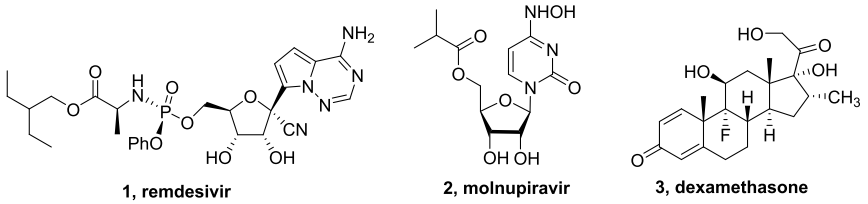

ACTT-1 enrolled 1062 patients, half who received remdesivir treatment on top of standard of care and half who received standard of care only.[6] Those who received remdesivir had a median recovery time of 10 days, compared with 15 days for those who received standard of care only. The patients who received remdesivir were also found to be more likely to have clinical improvement at day 15. The Kaplan−Meier estimates of mortality showed a trend toward improvement with remdesivir: mortality rates were 6.7% with remdesivir and 11.9% with placebo by day 15 and 11.4% with remdesivir and 15.2% with placebo by day 29. This trial was the basis for approval of remdesivir in the U.S. and Europe.

The SOLIDARITY trial, sponsored by the World Health Organization (WHO), studied four drug regimens: remdesivir, hydroxychloroquine, lopinavir/ritonavir, and interferon.[7] The study was conducted at 405 hospitals in 30 countries. A total of 11 330 adults were enrolled; 2750 were assigned to receive remdesivir, 954 to receive hydroxychloroquine, 1411 to receive lopinavir (without interferon), 2063 to receive interferon (including 651 to receive interferon plus lopinavir), and 4088 to receive no trial drug. The primary end point was mortality. Secondary outcomes were the initiation of mechanical ventilation and hospitalization duration. None of the drug regimens showed a positive effect on mortality, initiation of ventilation, or hospitalization duration.

On November 20, 2020, WHO issued a conditional recommendation against the use of remdesivir in hospitalized patients, regardless of disease severity, based on not only the SOLIDARITY trial but also other studies comprising approximately 7000 patients, where no meaningful effect was seen on mortality, the need for mechanical ventilation, the time to clinical improvement, and other clinical outcomes.[8]

Considering the differences in the outcomes of ACTT-1 and the SOLIDARITY trial, the authors of the SOLIDARITY trial suggested that in ACTT-1 there may have been a chance imbalance between the placebo and drug groups, with the proportion of lower-risk patients (those not already receiving high-flow oxygen or ventilation) appreciably greater in the remdesivir group than in the placebo group, therefore perhaps leading to improved outcomes.[7]

The ID Society points out that the two trials had many differences, as outlined in Table 1.[9] The primary end point for ACTT-1 was time to clinical improvement—it was not powered to determine an effect on mortality, although a trend was seen in reducing mortality. The SOLIDARITY trial was powered for mortality but was not designed to establish time to clinical improvement other than ventilated versus nonventilated. These variables may have played a role in the differing outcomes of the two trials.

Table 1. Differences between ACTT-1 and the SOLIDARITY Trial with Remdesivir

parameter	ACTT-1	SOLIDARITY
primary end point	time to clinical improvement	mortality
% ventilated patients enrolled	25%	8%
patients receiving concomitant glucocorticoids	25%	50%
time from symptom onset to randomization	median 9 days	no data
primary location of patients	80% North America, 15% Europe, 5% Asia	Asia, Africa, Latin America

A third clinical study examined the treatment of patients with moderate COVID-19 disease with remdesivir.[10,11] The trial, sponsored by Gilead, was an open-label study that examined 5 day and 10 day treatment periods. The study enrolled 584 patients at 105 hospitals in the U.S., Europe, and Asia.

https://doi.org/10.1021/acs.oprd.1c00100
Org. Process Res. Dev. XXXX, XXX, XXX−XXX

Participants were randomized in three groups, with 197 receiving a 10 day course of remdesivir, 199 receiving a 5 day course of remdesivir, and 200 receiving standard of care. Subjects had confirmed SARS-CoV-2 infection and were able to maintain an oxygen saturation greater than 94%. The primary end point was clinical status based on a seven-point scale. The 10 day treatment provided no benefit, while the 5 day treatment showed a modest but statistically significant improvement of clinical status relative to standard of care. The authors of this study aptly summarized the evidence to date regarding remdesivir treatment: many unanswered questions remain regarding the optimal use of remdesivir, including the appropriate patient population, duration of treatment, and use in combination with dexamethasone or other corticosteroids.

Regardless of the questions regarding efficacy, remdesivir is being used extensively in the U.S. In their earnings press release on February 4, 2021, Gilead noted that 50% of patients hospitalized for COVID-19 in the U.S. are being treated with remdesivir.[12]

1.2. Synthetic Routes to Remdesivir. At the time of our initial publication on synthetic routes to remdesivir in mid-2020,[3] only routes from Gilead had been published in journal articles or patent applications. In this section we describe recent publications and patent disclosures from Gilead and other contributors, including approaches to the key triazine fragment **4**, improvements in the glycosylation step, and asymmetric approaches.

1.2.1. Synthesis of Triazine 4. The synthesis of triazine fragment **4**, a key intermediate for the synthesis of remdesivir, has not been disclosed in the Gilead publications or patent applications. Four routes to the triazine have been published by other groups, two in the older literature and two recently.[13]

The first synthesis, requiring only two steps, was reported by Klein and co-workers in 1994 (Scheme 1).[14] 2-Pyrrolecarboxaldehyde was treated with hydroxylamine-*O*-sulfonic acid (3.5 equiv) and KOH in water to produce, after silica chromatography, the desired product **5** in 43% yield, in which both N-amination and conversion of the aldehyde to the nitrile had occurred, along with a 37% yield of 2-cyanopyrrole (**6**), where only conversion to the nitrile had occurred. No commentary was provided on any efforts to improve full conversion to **5**. Treatment of the chromatographed **5** with formamidine acetate in refluxing EtOH afforded formamidino compound **7**, which could be isolated. Alternatively, when the reaction was carried out with potassium carbonate, triazine **4** was generated and, after crystallizaton from water, isolated in 66% yield. The starting material, pyrrole-2-carboxylaldehyde, is readily available or can be synthesized from pyrrole, $POCl_3$, and DMF.[15]

Scheme 1. First Reported Synthesis of Triazine 4

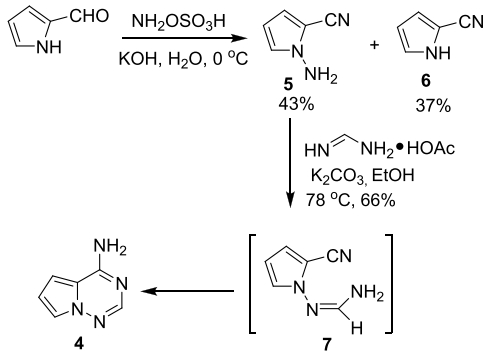

A four-step route to triazine **4** was published in a Bayer patent application in 2007 (Scheme 2).[16] 2,5-Dimethoxytetrahydrofuran (**8**) was reacted with *tert*-butyl carbazate in dioxane at 90 °C catalyzed by HCl. The reaction was driven to completion by distillation of MeOH. After aqueous workup, pyrrole **9** was crystallized from ether and isolated in 59% yield. In the next step, pyrrole **9** was reacted with chlorosulfonyl isocyanate in acetonitrile at 5 °C to generate *N*-chlorosulfonylamide intermediate **10**,[17] followed by addition of DMF with warming to room temperature. After aqueous workup and silica chromatography, nitrile **4** was isolated in 77% yield. The Boc group was then removed using HCl in dioxane. Aminopyrrole **6** was crystallized directly from the reaction mixture as its HCl salt by the addition of ether and isolated in 85% yield. The final step was carried out with formamidine acetate and potassium phosphate in EtOH at reflux. After aqueous workup and several manipulations, three crops of triazine **4** were isolated in a combined yield of 81%. The overall yield for the four step route was 31%.

Scheme 2. Bayer's Four-Step Route to Triazine 4

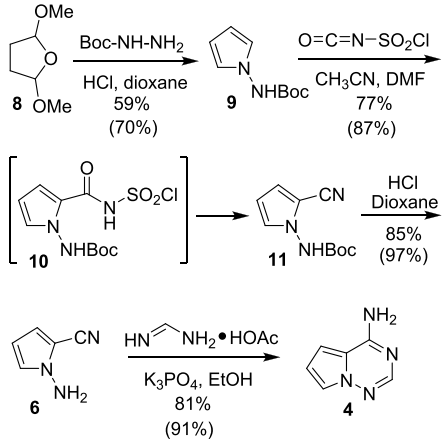

Bromination was also reported in the Bayer patent using 1,3-dibromo-5,5-dimethylhydantoin in DMF at −20 °C (Scheme 3).[16] The crude brominated product was isolated in 90% yield after aqueous workup and evaporation to dryness. Tituration in hot EtOAc afforded 57% recovery of the monobrominated product containing 2% of an undisclosed dibrominated byproduct. The conversion of triazine **4** to the iodo derivative has been described in Gilead patents using *N*-iodosuccinide in DMF at 0 °C.[18] The reaction was quenched into 1 M aqueous

Scheme 3. Bromination and Iodination of Triazine 4

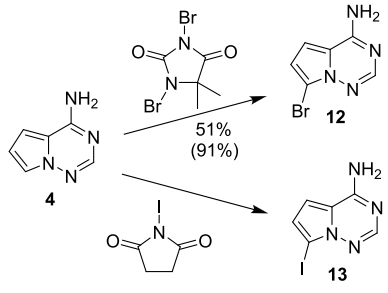

https://doi.org/10.1021/acs.oprd.1c00100
Org. Process Res. Dev. XXXX, XXX, XXX−XXX

NaOH, resulting in precipitation of the product. Filtration and drying afforded iodotriazine **13**. No yield was provided.

Neither of the first two routes were further developed for larger-scale implementation at the time they were reported. However, the Bayer route (Scheme 2) has been reproduced in a 2020 Chinese patent application, with each step reported on a 1 kg scale with minor modifications to the Bayer procedures.[19] The reported yields are given in parentheses under each reaction in Scheme 2, with an overall yield of 54% yield. Bromination was also reported to generate **12** in 91% yield (Scheme 3). The first step of the sequence, the conversion of **8** to **9**, was reported in a 2013 Almirall patent using HCl at 90 °C in NMP, with direct crystallization from the reaction mixture by addition of water to afford **9** in 89% isolated yield.[20] These two reports suggest that the Bayer route could likely be developed into a scalable route to support initial scale-up of remdesivir.

With large quantities required to support remdesivir commercial production, however, attention focused on more scalable routes from readily available raw materials. Snead and co-workers described a concise three-step route with only two isolations that provided triazine **4** in 54−58% yield using readily available and inexpensive starting materials (Scheme 4).[21] The

Scheme 4. Streamlined Route to Triazine 4

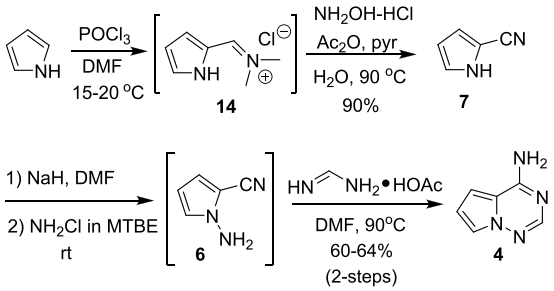

synthesis started from pyrrole with a one-pot, two-step introduction of the 2-nitrile group. First, reaction with DMF/$POCl_3$ generated iminium chloride **14**. Water was added to quench residual $POCl_3$, after which hydroxylamine hydrochloride, acetic anhydride, and pyridine were added and the mixture was heated to 90 °C for 16 h. The acetic anhydride served to activate the oxime formed in situ to afford an improved yield. After aqueous workup, the organic layer was concentrated, and 2-cyanopyrrole (**7**) was isolated by vacuum distillation in 90% yield. A possibility that may be worth considering is to incorporate and further optimize the work of Klein described in Scheme 1. Perhaps iminium salt **14** can be reacted with hydroxylamine-*O*-sulfonic acid to generate the *N*-amino bond and eliminate the iminium salt to the nitrile group to form **6**.

The next step in the Snead route involved direct amination with chloramine. Since neat chloramine is a gas and is unstable when concentrated, it is generally formed in situ as a dilute solution. Chloramine can be readily generated from ammonia and HOCl in water and extracted as a dilute solution in MTBE. A continuous stirred tank reactor (CSTR) system was devised to generate NH_2Cl in MTBE, which was fed into a solution of 2-cyanopyrrole and NaH in DMF to afford **6** with 93% conversion. The next step was carried out in the same reaction vessel by addition of formamidine acetate and warming to 90 °C for 16 h. Concentration of the reaction mixture followed by crystallization upon addition of water afforded triazine **4** in 60−64% yield. The authors addressed the reported hazardous use of NaH in DMF for the amination reaction by exploring other bases (KO-*t*-Bu and NaO-*t*-Bu) and glyme solvents, which were able to afford conversions in the 80−90% range under the best conditions. The authors also noted that they planned a follow-up publication with additional calorimetric data to support the use of NaH in DMF. Overall, this is a concise route that uses very inexpensive raw materials and an innovative continuous process to generate and use chloramine.

An approach to triazine **4** with different bond disconnections was recently published by the groups of Sarpong and Garg (Scheme 5).[13] The key step is an electrophilic aromatic

Scheme 5. Alternate Route to Triazine 4

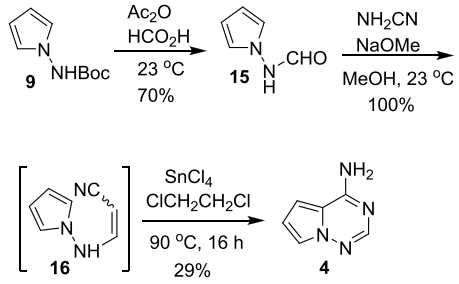

substitution of cyanoamidine **16** to produce triazine **4**. The route started with aminopyrrole **9**, which was formylated with acetic anhydride and formic acid to afford formamide **15** in 70% yield after silica chromatography. Reaction of **15** with cyanamide and sodium methoxide in MeOH afforded a mixture of cyano *E*/*Z* isomers **16** in quantitative yield. A number of protic and Lewis acids were surveyed for the key bond construction. Boron trifluoride etherate (22%) and tin tetrachloride (29%) in dichloroethane at 90 °C were the best catalysts found, although the yields of **4** were low. Further optimization was not carried out.

1.2.2. Improving the Glycosylation Step in the Remdesivir Synthesis. Gilead disclosed several variations of the glycosylation step of the remdesivir synthesis that were reviewed in our previous article.[3] In their patent applications, the yields ranged from 25 to 60% under varying conditions.[22] The 2016 and 2020 patent applications described the use of other Lewis acids for the glycosylation step, including cerium chloride, ytterbium chloride, lanthanum chloride−lithium chloride, and neodymium chloride. The reactions were described on a 5 g scale, but no yields were provided.[18] In the 2020 Gilead publication, which was primarily focused on the cyanation step, the experimental section described an improved glycosylation step on a 282 kg scale that gave a yield of 69% using a stoichiometric amount of neodymium chloride.[23] No discussion was provided for this experiment or the development effort that led to the use of neodymium chloride.

Further insight into the potential role of neodymium chloride has come from the identification of impurities in the glycosylation reaction without neodymium chloride from the laboratories of Williams and Kappe as part of their research to develop a flow process for the glycosylation step (reaction of **13** with **17** to generate **18**; Figure 2).[24] The low-temperature exothermic organometallic reaction with long addition times in batch mode is well-suited for a flow application in view of the rapid heat transfer and temperature control that are possible in continuous mode. The five-feed process (Figure 2) was developed on a flow-plate microreactor with an overall residence time of <1 min at 20 °C with a modest yield of 47%. The flow

https://doi.org/10.1021/acs.oprd.1c00100
Org. Process Res. Dev. XXXX, XXX, XXX−XXX

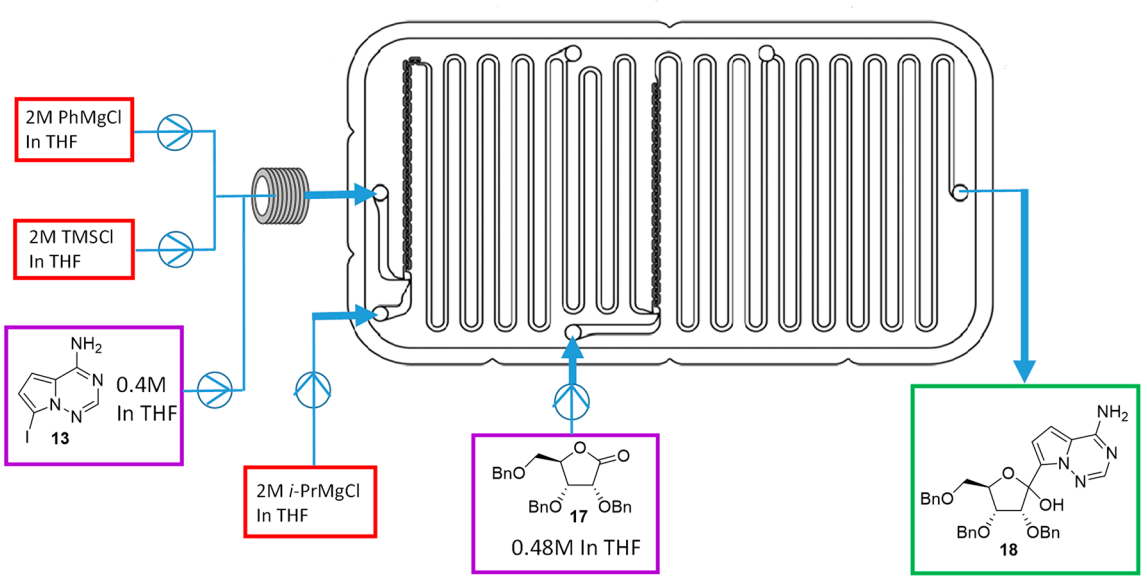

Figure 2. Flow reaction for the remdesivir glycosylation reaction[24]

sequence commenced with combining solutions of 2 M PhMgCl in THF (1.8 equiv) and 2 M TMSCl in THF (2.0 equiv). The resulting solution was then combined with triazine **13** as a 0.4 M solution in THF (1.0 equiv), with a residence time of 38 s, to generate the bis-silylated amine product. This mixture was introduced into the flow plate and combined with 2 M *i*-PrMgCl to effect Mg−I exchange, which was determined to require only 2.6 s. Finally, lactone **17** was fed into the flow plate, resulting in reaction to produce the coupled product **18** with a residence time of 9 s.[24]

While the yield is still lower than desired, this work has led to a better understanding of the reaction pathway and byproducts formed in the reaction, which may provide the basis for future yield improvement (Scheme 6). After bis-silylation using PhMgCl and TMSCl, Mg−I exchange is carried out using *i*-PrMgCl to generate carbanion **19-MgCl**. This carbanion then reacts with lactone **17** to form postulated ring-opened ketone **20**, which can undergo ring closure back to the lactone upon quench to afford the desired product **18** in 46.5% yield. The basic carbanion **19-MgCl** can also deprotonate lactone **17** to generate desiodotriazine **4**. This pathway accounted for 10.1% of the reaction mixture under the optimized conditions. Ketone **20** also undergoes secondary reactions, either with excess PhMgCl to form tertiary alcohol **21** (7.1%) or with additional **19-MgCl** to form bisaddition product **22** (12.7%).

The improved yield achieved by Gilead[23] using $NdCl_3$ is likely similar to the known effect of cerium(III) chloride to generate a less basic carbanion intermediate when used in conjunction with Grignard reagents.[26] The intermediate formed is unknown but proposed to be an RMgX−$CeCl_3$ complex.[26g] The less basic carbanion generated with the use of $NdCl_3$ could suppress deprotonation of lactone **17**. We also note that ketone **20** is more acidic than lactone **17**, so deprotonation of **20** could also occur under the conditions lacking $NdCl_3$, leading to potential epimerization or other undesired reactions.

A recent publication by Zhong, Qin and co-workers describes an improved glycosylation through the use of hindered secondary amines as stoichiometric additives (Scheme 7).[25] A number of amines were studied, and diisopropylamine provided the best yield of **18** (75% after isolation by column

Scheme 6. Reaction Pathway and Byproducts in the Glycosylation Reaction

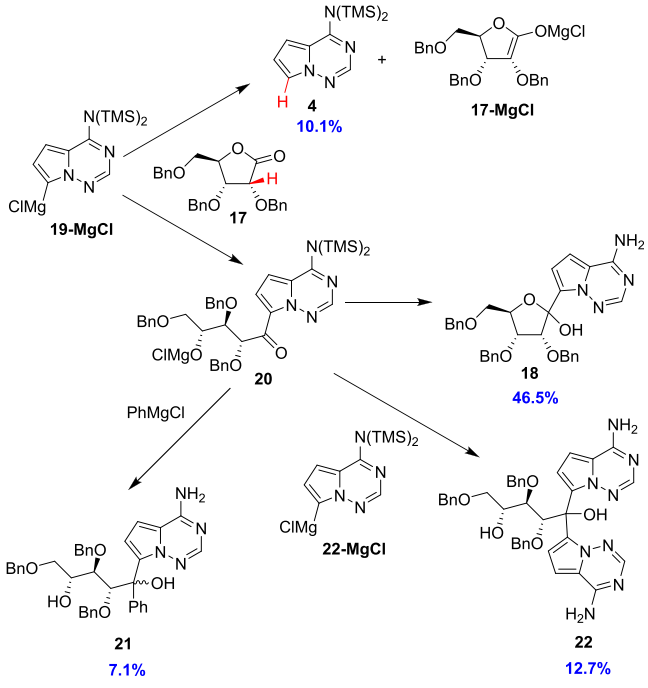

chromatography) on a 10 g scale at 0.08 M concentration. At scales of up to 180 g and 0.20 M, the yield was 62% after isolation by crystallization. The reaction was carried out in a single pot. Triazine **12** was first mixed with diisopropylamine (1.1 equiv) and 1,2-bis(chlorodimethylsilyl)ethane (**23**) (1.1 equiv) in THF at 20 °C, followed by cooling to −78 to −85 °C and slow addition of *n*-BuLi (4.3 equiv) to control the exotherm. This was followed by addition of lactone **17**, and the temperature was allowed to rise to −10 to 0 °C prior to quenching. The authors hypothesized that the amine may play two roles. First, it may facilitate silylation of the triazine amine to form **24**. In Scheme 7 we show silylation occurring during the first addition, but it may not occur until a portion of the *n*-BuLi has been added. Second,

https://doi.org/10.1021/acs.oprd.1c00100
Org. Process Res. Dev. XXXX, XXX, XXX−XXX

Scheme 7. Hypothesized Pathway for Improved Glycosylation of Lactone 17 using *i*-Pr$_2$NH

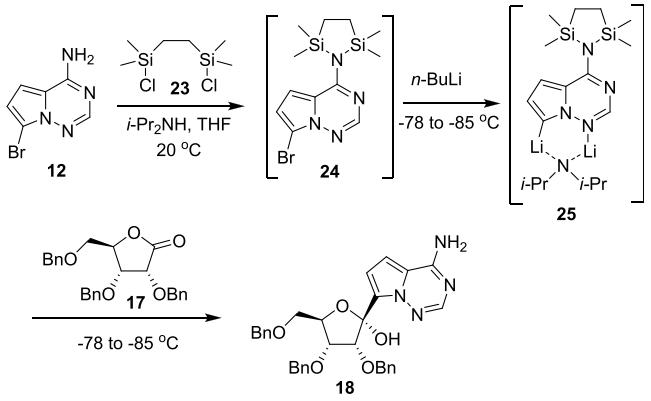

the amine may coordinate after lithiation to generate **25**, which may lead to improved selectivity (Scheme 7).

1.2.3. Alternate Protecting Group for the Phosphorylation Step. In the reported route to remdesivir from Gilead, the conversion of **26** to remdesivir entailed protection of the diol as acetonide **27** (90% yield), coupling with the single diastereomer of the *p*-nitrophosphate side chain (**28-*Sp***) to generate protected remdesivir (70%), and finally deprotection with concentrated HCl to afford remdesivir (**1**) in 69% yield (Scheme 8). The overall yield for the three-step process was 43%.[27]

Scheme 8. Gilead Final Steps to Remdesivir

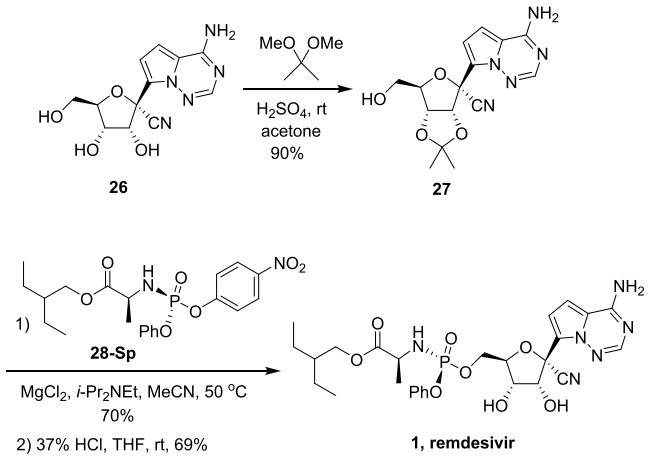

An alternate protecting group and coupling with the pentafluorophenyl side chain in 76% yield was reported by Hu, Shen, and co-workers (Scheme 9).[28] Triol **26** was treated with dimethylformamide dimethyl acetal (DMA-DMF) in pyridine as the solvent to generate **29**. After concentration to dryness and dissolution of **29** in THF, **30-*Sp*** was added, and the solution was cooled to −15 °C. MeMgBr was added, and then the solution was warmed to 0 °C and held at that temperature for 3 h. After aqueous workup and column chromatography that liberated the vicinal diol, **31** was isolated in 85% yield for the two steps. Deprotection of the amine was accomplished with HOAc in EtOH. After aqueous workup and column chromatography, remdesivir (**1**) was isolated in 90% yield.[28] While the yield was improved relative to the Gilead route, the authors did not elaborate on why they used the pentafluorophenyl side chain **30-*Sp*** instead of the 4-nitrophenyl side chain **28-*Sp*** used by Gilead.

Scheme 9. Alternate Protecting Group for the Final Steps of Remdesivir

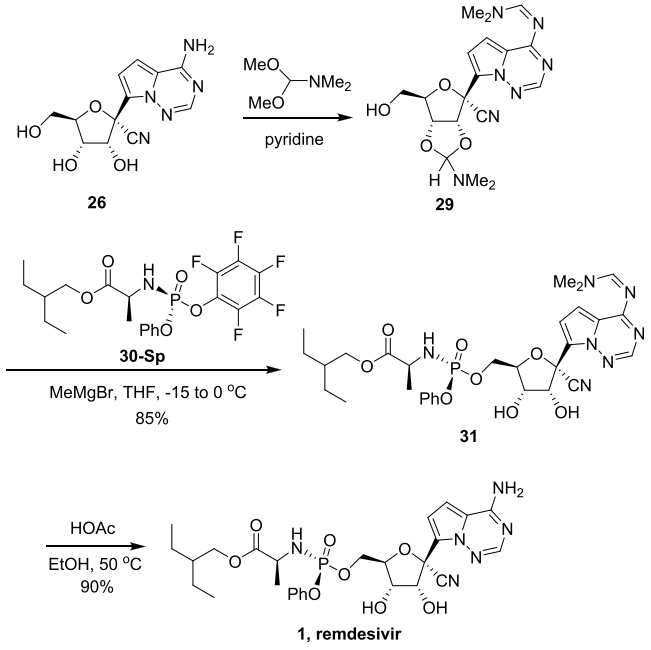

Perhaps the *p*-nitro group is not compatible with the Grignard reagent used for deprotonation of **29**. As discussed below, **28-*Sp*** can be isolated from a diastereomeric mixture by a dynamic kinetic crystallization process, making the Gilead route viable for scaling. It is unknown, and perhaps unlikely, that a similar crystallization process can be achieved with the pentafluorophenyl side chain. Nonetheless, the use of the alternate protecting group with a mild and high-yielding deprotection is an important contribution.

1.2.4. Asymmetric Synthesis of Remdesivir. In their 2017 publication on remdesivir, Gilead described two routes to the chiral phosphoramidate.[27] The first required chromatographic separation of the two diastereomers of **28**, while the second relied on the differential solubility of the isomers, which allowed selective crystallization of **28-*Sp*** from diisopropyl ether in 39% yield (Scheme 10).

Gilead also disclosed a crystallization-induced dynamic resolution of **28-*Sp*/*Rp*** to afford **28-*Sp*** (Scheme 11).[18] In the one-pot process, alanate ester **32** was reacted with phenyl dichlorophosphate and triethylamine at −20 °C in 2-PrOAc, followed by the addition of 4-nitrophenol and additional

Scheme 10. Second-Generation Phosphoramidate Process: Selective Crystallization of the *Sp* Diastereomer

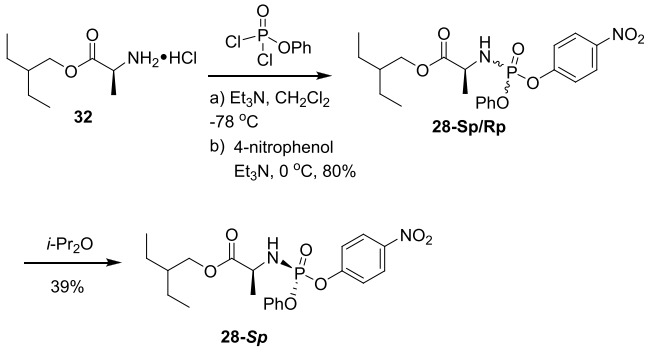

https://doi.org/10.1021/acs.oprd.1c00100
Org. Process Res. Dev. XXXX, XXX, XXX−XXX

Scheme 11. Third Generation of Phosphoramide Process: Crystallization-Induced Dynamic Resolution

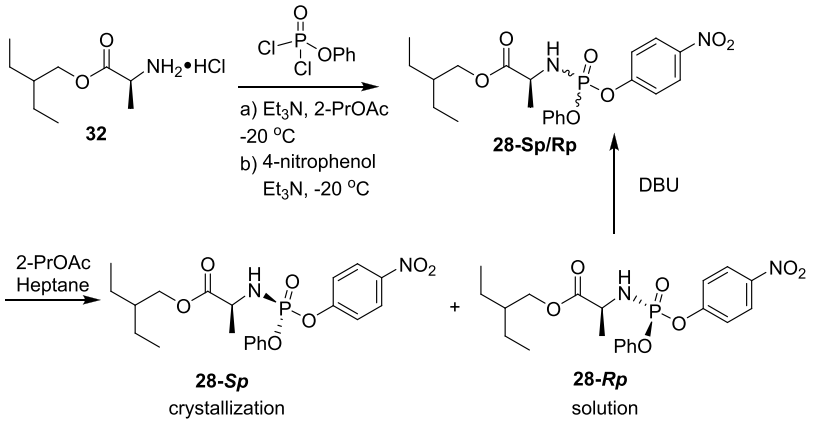

Scheme 12. Asymmetric Phosphorylation

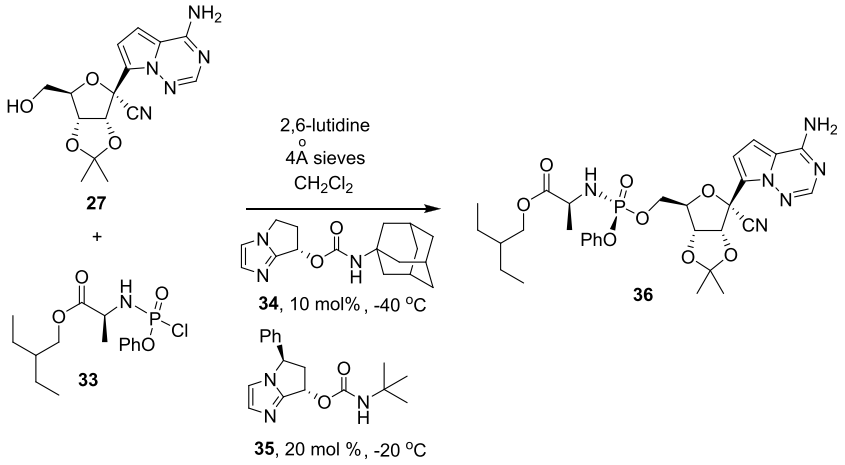

Scheme 13. Proposed DyKAT Pathway for Generation of 36-*Sp*

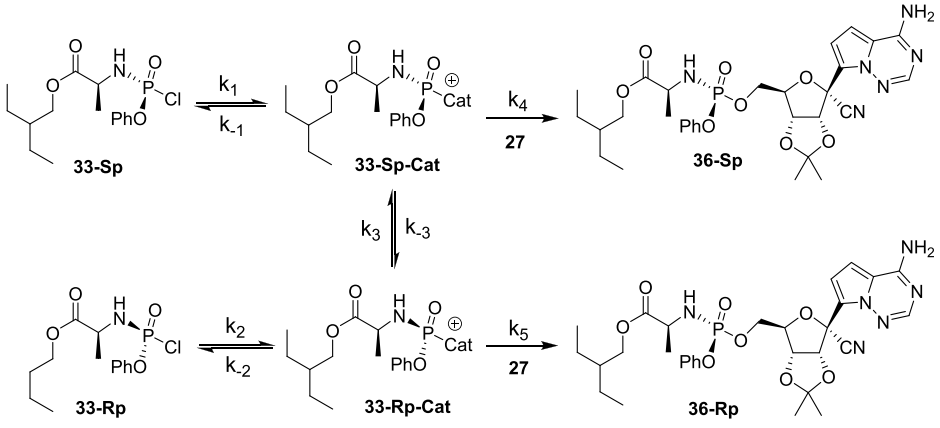

triethylamine. After quenching with aqueous HCl followed by carbonate and brine washes, the organic layer was concentrated, and then heptane was added along with seeding to induce crystallization. On the basis of the previous disclosure that the *Sp* diastereomer is less soluble than the *Rp* diastereomer, we presume that the seed and the crystallized product were the *Sp* isomer. The mixture was then treated with 10 mol % 1,8-diazabicyclo[5.4.0]undec-7-ene (DBU) for 21 h at 0 °C. After filtration and slurry in water, **28-*Sp*** was isolated. No yield was provided, but on the basis of their description of the process as a crystallization-induced dynamic resolution, we presume that DBU epimerized the *Rp* isomer in solution, while crystallization of the *Sp* isomer would ultimately drive the conversion to provide a high yield of **28-*Sp***.

Two asymmetric approaches to remdesivir were recently reported by Zhang and co-workers[29] and Wong, Hung, and co-workers[30] involving the use of a chiral catalyst to effect a diastereoselective phosphorylation via a dynamic kinetic asymmetric transformation (DyKAT) (Scheme 12). These two groups independently devised and developed similar chiral imidazole catalysts, **34** and **35**. In the publication by Zhang,[29] the reaction of alcohol **27** with phosphoryl chloride **33**, as a

https://doi.org/10.1021/acs.oprd.1c00100
Org. Process Res. Dev. XXXX, XXX, XXX−XXX

diastereomeric mixture at phosphorus, was carried out at −40 °C for 48 h in dichloromethane with 2,6-lutidine, 4 Å molecular sieves, and a 10% loading of imidazole catalyst **34**. The reaction on a 10 g scale afforded **36** with 95:5 diastereomeric ratio (dr). Crystallization afforded **36** with 99:1 dr in 85% overall yield. In the publication by Wong and Hung,[30] the reaction was carried out on a 1 g scale at −20 °C in dichloromethane with 2,6-lutidine, 4 Å molecular sieves, and a 20% loading of imidazole catalyst **35**. After completion of the reaction, the dichloromethane was evaporated, and the residue was treated with *p*-TsOH in MeOH to remove the isopropylidine group and generate crude remdesivir with 96:4 dr. After chromatography and crystallization from dichloromethane/acetonitrile, pure remdesivir was obtained in 74% yield with 99.4:0.6 dr.[30]

The reaction pathway proposed by Zhang involves a DyKAT, as outlined in Scheme 13.[29] The process depends on rapid epimerization (k_3/k_{-3}) of the phosphorus center of the two diastereomers, **33-*Sp*-Cat** and **33-*Rp*-Cat**, after displacement of the chloride with the catalyst. The slow and irreversible stereodiscriminating step is the reaction with **27**, wherein k_4 is significantly larger than k_5, affording **36-*Sp*** with high dr.

1.2.5. Summary of Remdesivir Synthetic Routes. Highlights from recent work toward the synthesis of remdesivir include the following:

- The three-step route to triazine **4** from simple raw materials developed by Snead and co-workers appears to be viable for development into a low-cost, green route to this important intermediate.
- The glycosylation remains a difficult reaction to control, but advances have been made in understanding and improving the reaction. Additional development of a continuous process for this step could prove worthwhile for this cryogenic reaction, where control of addition times, residence times, and temperatures are critical.
- The crystallization-induced dynamic resolution of the remdesivir phosphoramide developed by Gilead (Scheme 11)[18] provides straightforward access to this key chiral intermediate.
- Two similar organocatalytic asymmetric routes were developed. For these routes to be economical, the catalyst loadings will need to be further optimized from the current 10−20% levels.
- The use of an alternate diol protecting group derived from DMA-DMF is worth pursuing given its ease of removal relative to the isopropylidene group, which likely would minimize degradation during the deprotection step.

2. MOLNUPIRAVIR

Molnupiravir (**2**, EIDD-2801, MK-4482) is an orally active antiviral prodrug candidate that was discovered at Emory University. The active metabolite, β-D-N^4-hydroxycytidine (NHC, **37A**/**37B**) (Figure 3), was originally targeted for the treatment of hepatitis C (HCV) in the early 2000s.[31] Molnupiravir has shown broad-spectrum activity against several RNA viruses, including influenza A and B, Ebola, norovirus, RSV, HCV, coronavirus, and Venzuelan equine encephalitis virus (VEEV). With the emergence of SARS CoV-2 in early 2020, focus rapidly shifted to the evaluation of molnupiravir for the treatment of SARS CoV-2.[32]

β-D-N^4-Hydroxycytidine acts by disrupting RNA synthesis. Incorporation of the molecule during viral RNA synthesis leads to subsequent base-pair misreading, resulting in high mutation

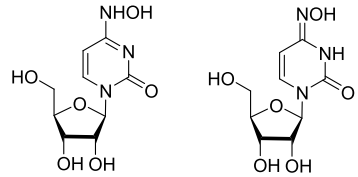

37A hydroxylamine tautomer **37B** oxime tautomer

Figure 3. Structures of NHC tautomers.

rates and ultimately genome lethality.[33,34] NHC exists as two tautomeric forms that have been shown to have similar energies in aqueous solution (Figure 3).[35] A theoretical study suggested that the oxime tautomer **37B** may base-pair with uracil (U), adenine (A), and guanine (G) while the hydroxylamine tautomer **37A** mimics cytosine (C), which base-pairs with G, resulting in an assortment of mutations.[35] In a study that examined the effect of NHC on viral guide RNA synthesis in VEEV, 8.9 mutations per 10 000 nucleotides were identified in media containing NHC versus only 0.85 mutations per 10 000 nucleotides in the control medium, a >10-fold increase. The majority of the mutations were transition mutations, with 4-fold more U-to-C or C-to-U than A-to-G or G-to-A.[34] Molnupiravir has also been shown to have potent activity against SARS CoV-2 that is resistant to remdesivir.[32] Oral treatment of molnupiravir to mice[32] and ferrets[36] infected with COVID-19 was effective in reducing viral load in the upper respiratory tract and in blocking transmission of the virus to untreated contact animals.

The rights to molnupiravir were acquired by Ridgeback Biotherapeutics, which is now partnering with Merck to advance clinical trials for the treatment of SARS CoV-2.[37] In October 2020, Merck initiated a Phase 2/3 trial in hospitalized patients with doses of 200, 400, and 800 mg twice daily for 5 days. with a target enrollment of 1300 patients.[38] In March 2021, Merck and Ridgeback announced preliminary results from a Phase 2a study in 207 patients.[39] The results of the primary end point, a reduction in time to viral negativity, were not disclosed. A secondary end point showed a reduction in time to negativity of infectious virus in nasopharyngeal swabs in patients with SARS-CoV-2 infection.

2.1. Synthetic Routes to Molnupiravir. Several routes to molnupiravir have been published, most of them very recent, indicating the high level of interest in this molecule as a potential treatment for COVID-19. This section is divided into three parts based on the primary starting materials used for the route: uridine, cytidine, and ribose.

2.1.1. Routes to Molnupiravir Starting from Uridine. The original synthesis of molnupiravir was reported on a 25 g scale in a 2019 patent from Emory University and involved five steps from uridine (**38**) (Scheme 14).[40] In the first step, the vicinal diol was protected using acetone and sulfuric acid at room temperature for 18 h to generate acetonide **39**. The reaction mixture was neutralized with trimethylamine, and then triethylamine and 4-(*N*,*N*-dimethylamino)pyridine (DMAP) were added. The reaction mixture was cooled to 0 °C, and isobutyric acid anhydride was slowly added, after which the mixture was allowed to warm to room temperature. After aqueous workup, the organic layer was concentrated to provide ester **40** as an oil in 99% yield uncorrected for purity. Crude **40** was dissolved in acetonitrile, and then 1,2,4-triazole (7 equiv) and triethylamine (8 equiv) were added. The solution was cooled to 0 °C, treated with $POCl_3$ (1.5 equiv), and allowed to warm to room

https://doi.org/10.1021/acs.oprd.1c00100
Org. Process Res. Dev. XXXX, XXX, XXX−XXX

Scheme 14. Original Synthesis of Molnupiravir from Uridine

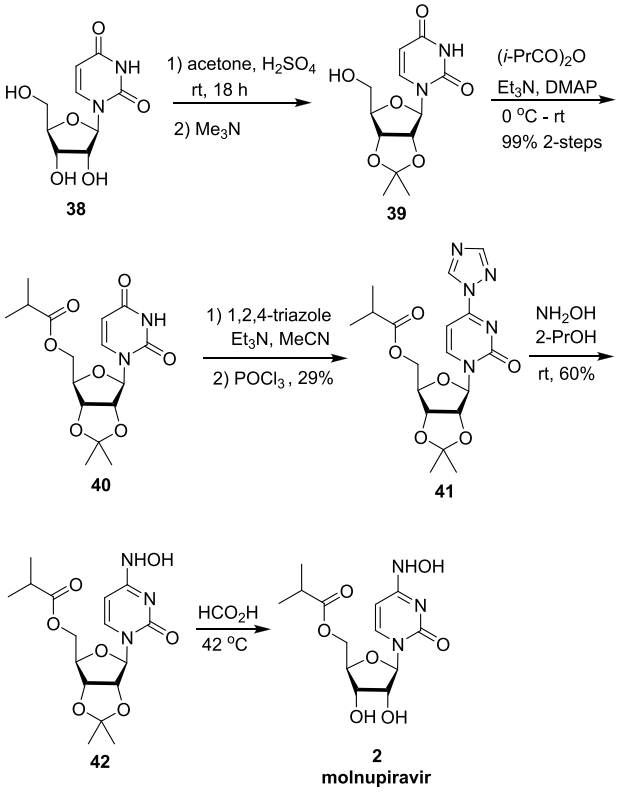

temperature. After aqueous workup and flash chromatography, triazole **41** was isolated in 29% yield. Triazole **41** was dissolved in 2-PrOH and treated with hydroxylamine at room temperature. After aqueous workup and concentration, **42** was isolated in 60% yield as an oil that slowly converted to crystalline material. Deprotection was carried out in neat formic acid at room temperature, followed by concentration at 42 °C to afford molnupiravir (**2**) as an oil. Crystallization and recrystallization were carried out using 2-PrOH/MTBE. No yield was provided for this step.[40]

An alternate route from uridine devised by Kappe, Dallinger, and co-workers involves the same five transformations as the original route, but in different order and with a much-improved yield (Scheme 15).[41] The key deficiency in the original route was the 29% yield in the triazole insertion step. In the revised route, the triazole insertion was carried out as the first step using a modification of the procedure reported by Miah and co-workers.[42] The process involved in situ TMS protection of the hydroxy groups, insertion of the triazole group via activation with $POCl_3$ and 10 equiv of 1,2,4-triazole, and deprotection of the TMS groups using HOAc/MeOH. Use of lesser amounts of 1,2,4-triazole resulted in lower yields. Triazole **38** precipitated from the reaction mixture and was isolated in 88% yield, which is a significant improvement over the 29% yield of the first-generation route. Protection of the vicinal diols was carried out next using 2,2-dimethoxypropane catalyzed by 5 mol % sulfuric acid in acetonitrile. After completion of the reaction, the MeOH produced from acetonide formation was removed by azeotropic distillation, and then isobutyric acid anhydride, triethylamine, and catalytic DMAP (25%) were added, furnishing isobutyl ester acetonide **41** in quantitative yield after extractive workup for the two-step, one-pot process. Conversion of the triazole group to hydroxylamine functionality was carried out by treating **41** with

Scheme 15. Alternative Five-Step Route to Molnupiravir from Uridine

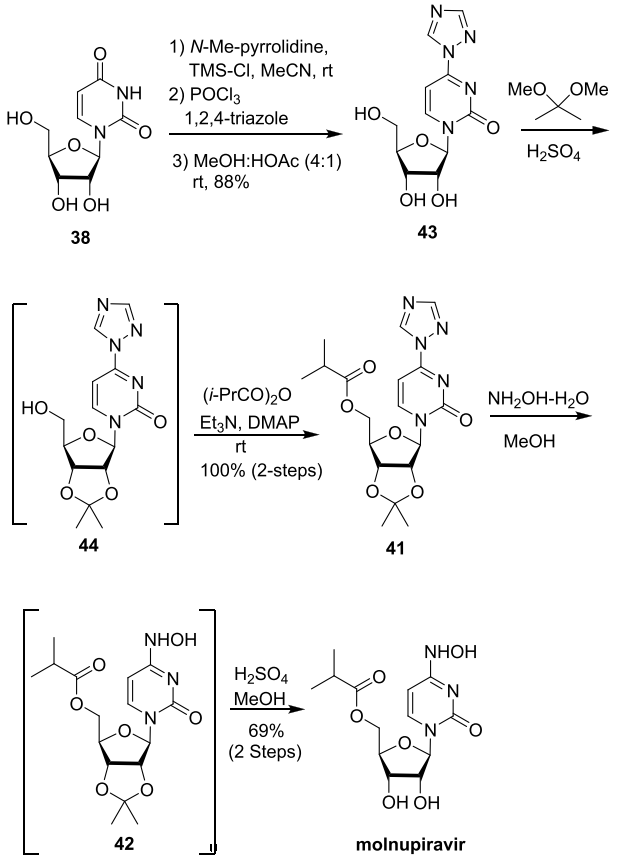

hydroxylamine (50 wt % in water) for 20 min followed by extractive workup to provide **42** in 90% yield with 91% purity by HPLC. A flow system was designed to control the exotherm and minimize hydrolysis byproducts in the final deprotection step. The optimized flow deprotection was carried out in MeOH with 2.75 equiv of sulfuric acid at 100 °C with a residence time of 5 min, providing 79% conversion along with an 11% yield of the ester hydrolysis product NHC (**37**) and an 8% yield of the hydroxylamine hydrolysis product (the isobutyl ester of uridine). Chromatographic isolation afforded molnupiravir in 69% isolated yield from **41** on a 300 mg scale. The overall yield for the five-step process was 61%.[41] This process was a significant improvement over the original route and could likely be scalable if the final deprotection step could be further optimized such that molnupiravir could be isolated and purified by crystallization.

2.1.2. Routes to Molnupiravir Starting with Cytidine. Snead and co-workers published a four-step route to molnupiravir starting with cytidine (**45**) (Scheme 16).[43] The synthesis began with formation of the acetonide using 2,2-dimethoxypropane in acetone with sulfuric acid as the catalyst. Acetonide **46**, as its sulfuric acid salt, precipitated from the reaction mixture and was isolated in 98% yield. Reaction with isobutyric acid anhydride using DBU and catalytic DMAP in acetonitrile afforded ester **47** in 78% yield after flash chromatography. Hydroxyamination was carried out in 70% aqueous 2-PrOH using hydroxylamine sulfate at 72−73 °C to afford product **42** in 96% yield after workup. Acetonide deprotection was conducted in formic acid at room temperature. After flash chromatography, molnupiravir was isolated in 60% yield with 98% purity. Alternatively, the

https://doi.org/10.1021/acs.oprd.1c00100
Org. Process Res. Dev. XXXX, XXX, XXX−XXX

Scheme 16. Three- and Four-Step Routes to Molnupiravir from Cytidine

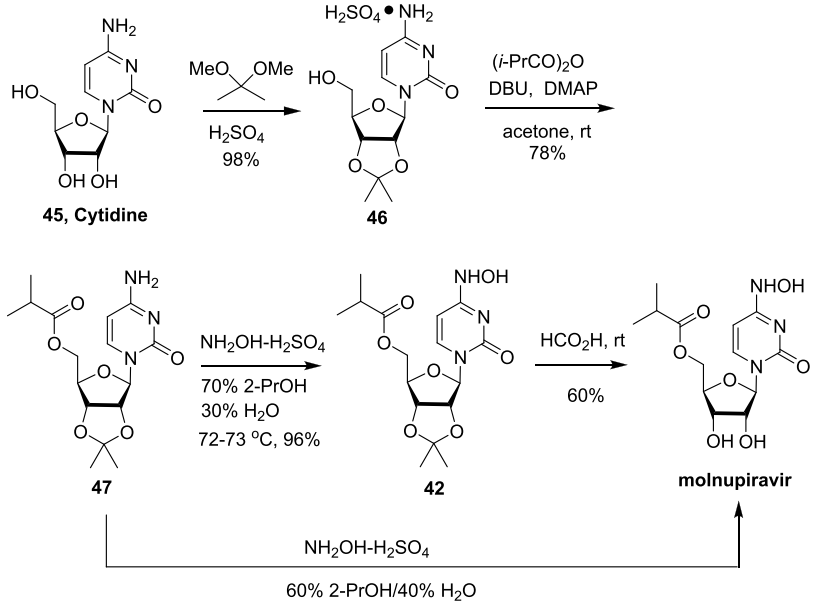

Scheme 17. Two-Step Routes to Molnupiravir from Cytidine

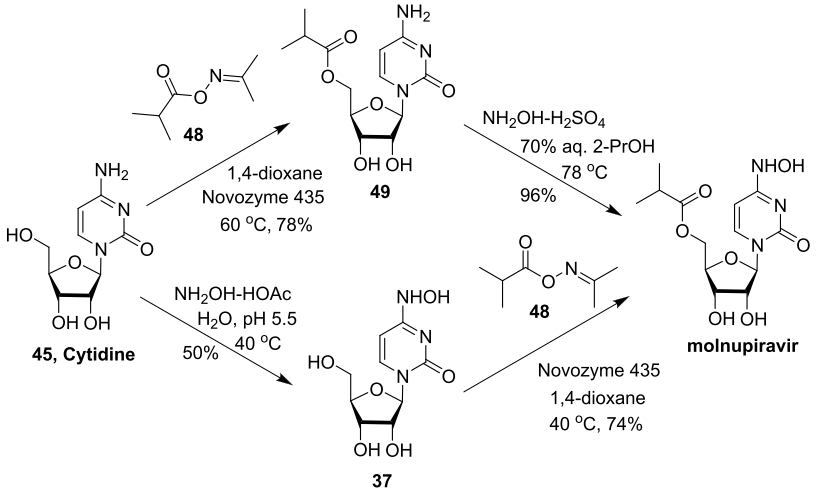

hydroxyamination and deprotection of **47** could be carried out in the same pot simply by extending the hydroxyamination step by 1 h (from 17 to 18 h) and increasing the water content of the solvent mixture from 30% to 40%. However, 20% ester cleavage occurred under these conditions with an isolated yield of 53%. The overall yield was 41% by the three-step route or 44% for the four-step route.

Snead and co-workers also published two different two-step routes from cytidine (Scheme 17).[44] The two transformations consist of installation of the isobutyl ester and hydroxyamination, which can be conducted in either order. Selective enzymatic esterification of the primary alcohol eliminated the diol protection/deprotection sequence required with the previous routes. Starting with cytidine allowed for a one-step transamination, eliminating the activation step required for installation of the hydroxylamine when starting with uridine.

Hydroxyamination of cytidine to generate **37** was accomplished using the acetic acid salt of hydroxylamine in water at 40 °C for 48 h (Scheme 17). At the end of the reaction, the solvent was removed by rotary evaporation to give a syrup that was crystallized from water to provide **37** in 50% yield. Alternatively, hydroxyamination could be carried out as the second step. Hydroxyamination of cytidine isobutyryl ester **49** was a higher-yielding reaction with use of $NH_2OH{\cdot}H_2SO_4$ in i-PrOH for 20 h at 78 °C, affording molnupirvair in 96% isolated yield after column chromatography.

Selective enzymatic acylation of the primary hydroxy group was achieved using Novozyme 435 (immobilized *Candida antarctica* lipase B) for both cytidine and **37**. Isobutyric oxime ester **48** was used as the acyl transfer agent with solid-supported enzyme (200 wt %, 1.5 mol %) using 1,4-dioxane as the solvent. The reaction with cytidine was carried out with 5 equiv of oxime ester **48** at 60 °C for 43 h. Filtration to remove the enzyme, solvent evaporation, and column chromatography afforded **37** in 78% yield. Enzymatic reaction with **37** was carried out for 2 h at 40 °C with 3 equiv of oxime ester to provide molnupiravir in 74% yield after column chromatography.

When the esterification was conducted first, molnupiravir was obtained in 75% yield, and when the hydroxyamination was conducted first, the yield was 37%. While these approaches are

https://doi.org/10.1021/acs.oprd.1c00100
Org. Process Res. Dev. XXXX, XXX, XXX−XXX

attractive from a step-count perspective, the authors raised concerns that the expense of oxime ester **48** and the immobilized enzyme, which is used in large amounts, could limit its usefulness as a commercial route.[44] In an update from the Jamison group posted on ChemRxiv, the two-step route shown on the upper portion of Scheme 17 has been further developed into a scalable route with no chromatographies in 41% overall yield (Scheme 18).[45]

Scheme 18. Developed Two-Step Route to Molnupiravir

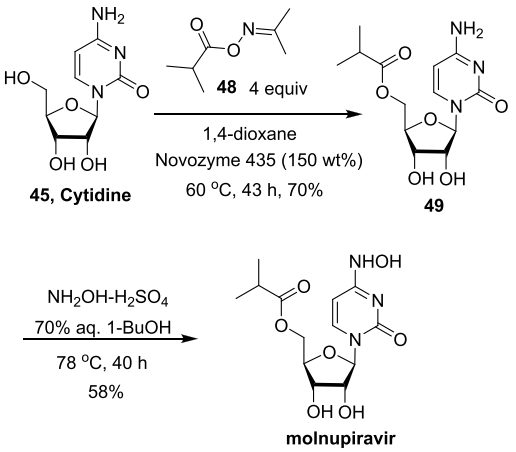

Few changes were made to the chemistry, but crystallizations were developed for both steps. Although an extensive solvent screen was carried out, 1,4-dioxane proved to be optimal for the first step, and the enzymatic reaction required high dilution (2 g/L). The enzyme loading was reduced from 200 wt % to 150 wt %, and the amount of **48** was reduced from 5 to 4 equiv. The product was crystallized from acetone in an overall yield of 70%. For the second step, the solvent mixture was changed from 70% aqueous 2-PrOH to 70% aqueous 1-BuOH. Molnupiravir was isolated in 58% yield with 97 wt % purity after crystallization from water. No details were provided on the reaction yields and the recoveries for the crystallizations from both steps, but there appears to be room for further improvement in the crystallization yields, especially for the second step, where the reported yield in Scheme 17 was 96%.

TCG GreenChem, who coauthored the paper, provided a raw material cost estimate for the route in the Supporting Information for ref 45. Major cost drivers were cytidine ($57/kg) and Novozyme 435 ($50/kg). On the basis of a simplified process for the preparation of oxime ester **48**, a raw material cost estimate of $16.37/kg was calculated for this compound. The overall cost of molnupiravir based on raw materials only was calculated to be $799/kg with no solvent recycling and $427/kg with solvent recycling, assuming 75% recovery. Clearly, increasing the yields could lower the raw material costs substantially. These estimates do not include labor and overhead. If we apply an estimate of $50/kg per step for the two non-GMP steps to manufacture oxime ester **48** and $100/kg for the two GMP steps to manufacture molnupiravir, a ballpark cost is estimated to be $727/kg with solvent recycle. Assuming the highest dose (1600 mg/day) studied in the ongoing clinical trial, the cost of manufacture per patient day would be $1.17. For the maximum treatment period of 10 days, the cost of manufacture per patient treatment would be $11.70.

A team from Manchester University led by Lovelock, Turner, and Green developed a biocatalytic route to *N*-hydroxycytidine from cytidine using cytidine deaminase (Scheme 19).[46] The natural enzyme catalyzes the aqueous deamination of cytidine

Scheme 19. Biocatalytic Conversion of Cytidine to *N*-Hydroxycytidine

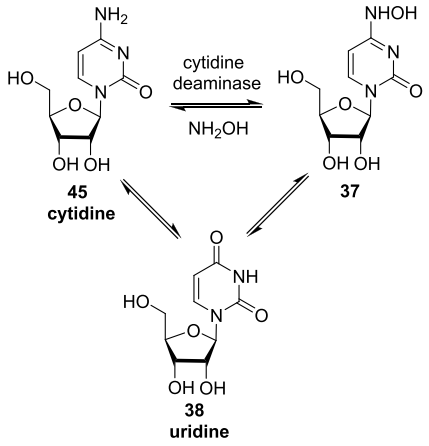

(**45**) to uridine (**38**). When 50% aqueous hydroxylamine is used as the solvent, the reaction provides up to a 6:1 *N*-hydroxycytidine/uridine mixture. A two-step enzymatic process from cytidine could be envisioned if the deaminase reaction could be further optimized to provide higher yields of *N*-hydroxycytidine (**37**), followed by selective enzymatic esterification of the primary alcohol as demonstrated by the Snead team (Scheme 17).

Aisa, Shen, and co-workers reported a four-step synthesis of molnupiravir from cytidine in 70% yield with only a single isolation at the end (Scheme 20).[28] This route uses DMF-DMA to protect the diol and to activate the amine. The synthesis started with treatment of cytidine with DMF-DMA using pyridine (10 equiv) in THF to afford crude **50** after concentration to dryness. Addition of dichloromethane, isobutyric acid anhydride, triethylamine, and DMAP (5 mol %) at room temperature afforded ester **51**. When the reaction was complete, EtOH was added, resulting in deprotection of the diol to generate **52**. After evaporation to dryness, 70% *i*-PrOH/water and hydroxylamine sulfate were added, and the reaction mixture was heated to 78 °C for 18 h. After cooling to room temperature, the resulting two layers were separated. The organic layer was concentrated to dryness, and then molnupiravir was crystallized from 2-methyltetrahydrofuran followed by a reslurry in 2-PrOAc in an overall yield of 70%. The use of DMF-DMA as a protecting group is attractive since it can be readily removed without hydrolysis of the ester. Further development for solvent exchanges between steps without concentration to dryness could provide a high-yielding, scalable route to molnupiravir.[28]

2.1.3. Route to Molnupiravir from Ribose. As noted above, Merck is working with Ridgeback in conducting late-stage clinical trials for molnupiravir in COVID 19 patients. Merck and Codexis recently deposited a non-peer-reviewed manuscript in ChemRxiv that describes a three-step route to molnupiravir from readily available raw materials (Scheme 21).[47] Merck chose to start with the very inexpensive raw material ribose instead of cytidine or uridine, which they noted were expensive and perhaps not available on the scale expected to be required.

The three-step route starts with the biocatalytic esterification of ribose (**53**). The proof of concept was achieved using oxime

https://doi.org/10.1021/acs.oprd.1c00100
Org. Process Res. Dev. XXXX, XXX, XXX−XXX

Scheme 20. Four-Step Single-Isolation Route to Molnupiravir

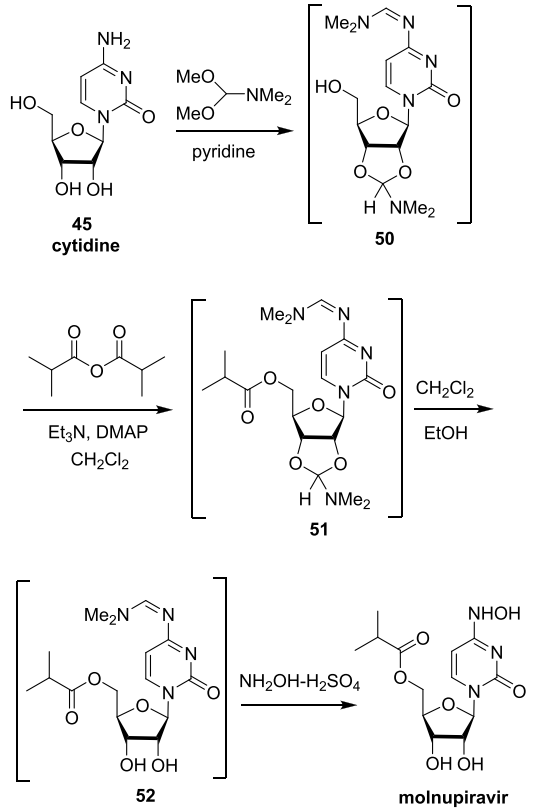

Scheme 21. Potential Manufacturing Route to Molnupiravir

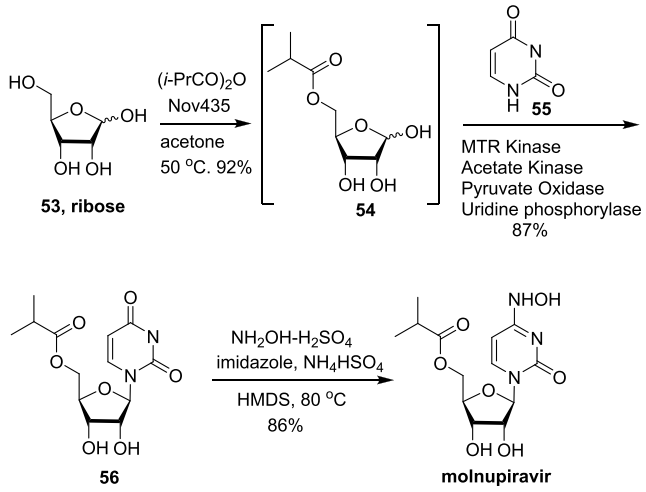

ester **48** with a number of lipases in an organic solvent. The optimized conditions were the use of a 10 wt % loading of the immobilized enzyme Novozyme 435 in acetone at 50 °C with isobutyric acid anhydride instead of **48** as the ester donor, which afforded ester **54** in 94% yield with minimal diester byproducts. The ester was difficult to isolate given its high water solubility and poor crystallinity. As such, since the subsequent biocatalytic step would be carried out in water, the decision was made to advance **54** as an aqueous solution. Workup consisted of filtration to remove the immobilized enzyme, solvent exchange to MTBE, and extraction of the product into water. Excess isobutyric acid anhydride and most of the isobutyric acid byproduct remained in the organic layer.

The introduction of uracil (**55**) required the invention of a new biocatalytic reaction involving multiple engineered enzymes (Scheme 22). Nucleoside phosphorylases catalyze

Scheme 22. Pathway for Enzymatic Conversion of 54 to 56

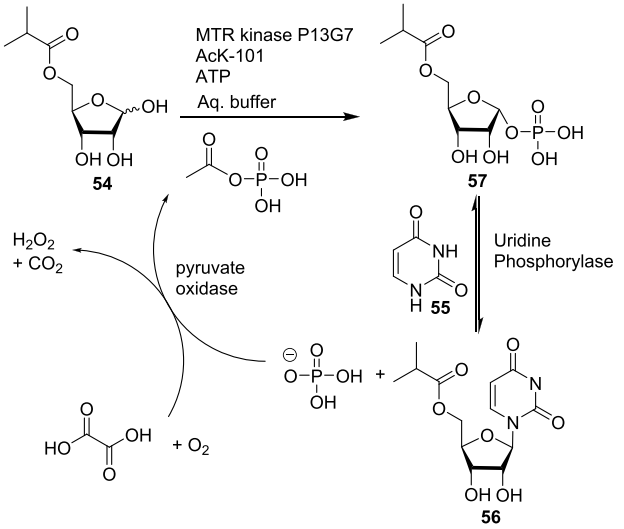

the reversible reaction between a sugar phosphorylated at the anomeric position and a nucleoside. Screening identified a uridine phosphorylase from *Escherichia coli*, optimized in a single round of engineered evolution, that effected the desired reaction between phosphate **57** and uracil with high conversion and low loadings. The next challenge was generation of phosphate **57**. Enzymatic phosphorylation generally occurs at a C5-hydroxy group that is subsequently isomerized to the anomeric position enzymatically followed by the biocatalytic reaction with the nucleobase. Since the 5-OH has been esterified, a direct phosphorylation at the anomeric center was required. No natural enzymes are available that phosphorylate at the 1-position and catalyze nucleoside biosynthesis. However, 5,5-methylthioribose kinases (MTKs) catalyze the desired phosphorylation, so a two-enzyme cascade process was envisioned, one for phosphorylation and one for nucleoside conversion. From a screening of natural enzymes, a phosphorylase from *Klebsiella* spp was selected for further engineering, ultimately resulting in an enzyme that could phosphorylate in the 1-position with 99% conversion and >99% dr for the desired α diastereomer. To recycle ATP, an additional enzyme was required, acetate kinase (AcK-101).

For conversion to the nucleoside **56**, enzyme engineering of a uridine phosphorylase from *E. coli* afforded an enzyme that catalyzed nucleobase formation with good activity. Since the nucleobase formation is reversible, yet another enzymatic system was required to remove inorganic phosphate. Instead of removing phosphate, the final strategy that was designed used the phosphate generated in the nucleobase formation to convert pyruvate to acetyl phosphate, which was then used for the phosphorylation at the 1-position. Overall, the step involves four enzymes: MTR kinase for phosphorylation, uridine phosphorylase for nucleobase formation, and pyruvate oxidase and Ack for regeneration of acetyl phosphate and ATP (Scheme 22). After the reaction was complete, the product **56** was extracted into 2-

https://doi.org/10.1021/acs.oprd.1c00100
Org. Process Res. Dev. XXXX, XXX, XXX−XXX

MeTHF, followed by crystallization from EtOAc/heptane in 87% yield.

The final step involved conversion of the amidic carbonyl group of **56** to the hydroxylamine. Activation of the ring was accomplished by silylation with catalytic imidazole, ammonium bisulfate, and hexamethyldisilazane, which was also used as the solvent, followed by reaction with hydroxylamine as its sulfuric acid salt. The initial product of the reaction was molnupiravir with both hydroxy groups bearing TMS groups, which allowed for removal of salts and inorganic byproduct by an aqueous wash, followed by deprotection via pH adjustment and then crystallization from EtOAc/MTBE to provide molnupiravir in 86% yield.[47]

2.1.4. Summary of Routes to Molnupiravir. Over the past several months, seven routes to molnupiravir have been published. All of them are significant improvements over the original medicinal chemistry route, although many of them have not been developed into practical routes with isolations via crystallization instead of chromatography. The innovative Merck/Codexis route has been developed into what appears to be a viable, low-cost commercial route.[47] The use of four engineered enzymes for the conversion of **54** to **56** brings up a question of cost, but the enzymes are used at low loadings ranging from 0.2 to 9 wt %. The Merck group appears poised to provide large quantities of drug should molnupiravir show efficacy, and therefore, Merck may not require manufacturing support from other companies/nations to meet worldwide demand.

The recent publication by Jamison and co-workers quotes a bulk price of cytidine at $57/kg,[45] so any of the short routes from cytidine could likely be developed into viable and reasonably low cost routes, as exemplified by the partially optimized Jamison route (Scheme 18).[45]

3. DEXAMETHASONE

Dexamethasone is a steroid that was first approved in 1959 and has been used primarily for treating inflammatory diseases and autoimmune disorders. The immunosuppressive and anti-inflammatory activity of dexamethasone is about 25-fold greater than those of other corticosteroid compounds, which has led to its study for dampening the excessive immune response seen in some COVID-19 patients, known as adult respiratory distress syndrome (ARDS).[48] Dexamethasone reversibly binds to several DNA sites, leading to inhibition of pro-inflammatory cytokines including interleukin IL-1, Il-2, Il-6, IL-8, TNF, IFN-γ, VEGF, and prostaglandins, several of which have been linked to ARDS caused by COVID-19. Dexamethasone also activates anti-inflammatory cytokine synthesis of IL-10 and lipocortin-1.[48]

A clinical study led by a team from Oxford University (UK RECOVERY trial) examined the effect of 6 mg of dexamethasone given once daily for 10 days in COVID-19 patients.[49] The study included 2104 patients on dexamethasone plus standard of care and 4321 patients treated with standard of care only. In the dexamethasone cohort, at day 28, mortality was reduced 35% in patients receiving mechanical ventilation and 20% in patients receiving supplemental oxygen. No benefit was observed for patients not receiving respiratory support at the time of randomization into the trial.[49] Patients in the dexamethasone group also had a slightly shorter duration of hospital stay (12 days vs 13 days). Patients in the dexamethasone group who were not receiving mechanical ventilation at the time of randomization were less likely to progress to mechanical ventilation, and those who were mechanically ventilated at time of enrollment were more likely to progress to cessation of ventilation.[49] In a second, smaller study of 299 patients with moderate or severe acute respiratory distress symptoms and COVID-19, standard of care treatment plus dexamethasone administered intravenously daily for 5 days at 20 mg followed by 5 days at 10 mg resulted in an increase of days free of mechanical ventilation (4.0 vs 6.6 days) over a 28 day period versus patients on standard of care only.[50]

On the basis of these studies, the U.S. National Institutes of Health has recommended the use of dexamethasone in hospitalized patients with COVID-19 who are on mechanical ventilators or need supplemental oxygen. Dexamethasone is not recommended for use in the early phase of the disease since its immune suppression activity may dampen the body's immune response to the virus.

3.1. Brief History of the Discovery of Dexamethasone.[51] In 1946, Sarett at Merck reported the first synthesis of cortisone, a monumental effort requiring nearly 40 steps.[52] Process chemists and chemical engineers at Merck developed a somewhat shorter and scalable process based on Sarett's work (Scheme 23)[53] and in 1948 provided a 100 mg sample to

Scheme 23. Merck Routes to Cortisone and Dexamethasone via Enone 59

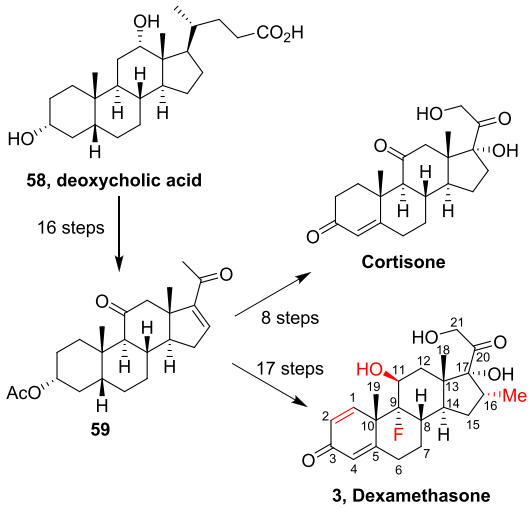

clinicians at the Mayo Clinic to treat a woman with severe arthritis. The results were dramatic—the crippling effects of the disease diminished within 2 weeks. A New York Times reporter gained access to an internal Mayo meeting and subsequently published sensational stories on the clinical success of cortisone.[54]

Cortisone was a remarkable breakthrough for medical research, but longer-duration treatment caused serious side effects. The story of patient #1 did not have a happy ending. Her intended treatment regimen was 50 mg of cortisone twice daily for 6 months. After a month, however, she had gained weight and had facial puffiness and erratic mood swings that resulted in her being admitted to a psychiatric hospital. Other early patients experienced similar side effects that are now well-known with steroid therapy.[54b,c] It became clear that cortisone could be an amazingly effective drug, but intolerable side effects would severely limit its use. The pharmaceutical industry began an effort to design a steroid with an improved therapeutic index and a longer half-life (cortisone has a half-life of 1−2 h in humans,

https://doi.org/10.1021/acs.oprd.1c00100
Org. Process Res. Dev. XXXX, XXX, XXX−XXX

Scheme 24. Merck Route to Dexamethasone from Enone 59

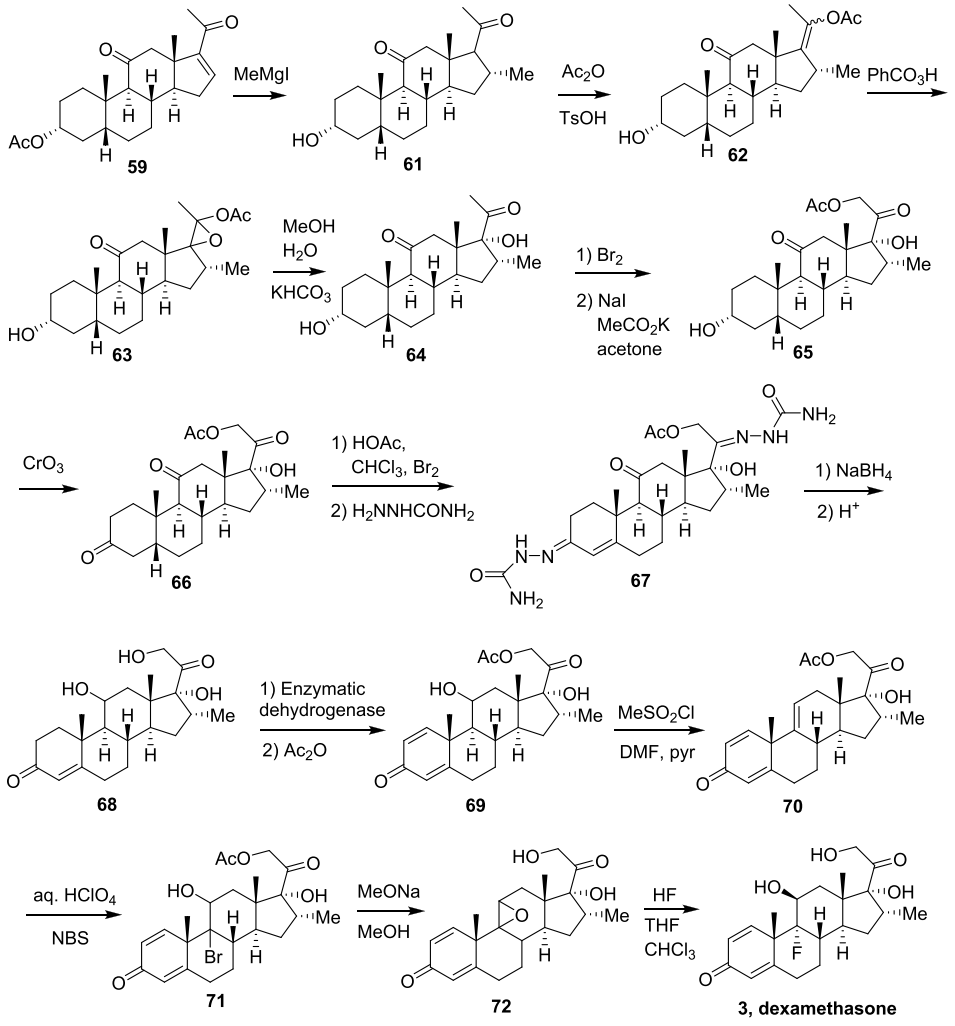

depending on the dose).[55] In 1953 and 1954, Fried and Sabo at Squibb reported that 9-α-halo derivatives of cortisone had enhanced glucocorticoid (anti-inflammatory) activity, with the α-fluoro analogue having a 10-fold increase in activity versus cortisone.[56] However, this analogue also increased the undesirable mineralocorticoid (salt retention) activity that was responsible for some of the cortisone side effects. Schering researchers discovered that the introduction of a C1−C2 double bond (prednisolone) increased the desirable anti-inflammatory activity 3-fold while reducing salt retention.[53] Meanwhile, efforts were underway at Merck to block metabolic activity at the C20 ketone by installing substituents at C16. These three modifications came together in dexamethasone (**3**), which was 25-fold more potent than cortisone, had a half-life of 36−54 h,[55] did not cause salt retention (minimal mineralocorticoid activity), and had an overall much-improved therapeutic index relative to cortisone (Scheme 23).[53]

3.2. Synthesis of Dexamethasone. Dexamethasone was commercialized by both Merck and Schering in 1959 under the brand names Decadron (Merck) and Deronil (Schering). In 1958, each company published a one-page communication with no structures describing their synthesis of dexamethasone. The starting material for the Merck route[57] was deoxycholic acid (**58**), a bile acid obtained from cattle. The Schering route[58] started with diosgenin (**60**), a material derived from yams. The early steps of each route were based on their respective syntheses of cortisone developed in the late 1940s and early 1950s. This section on synthetic routes to dexamethasone is divided into three parts on the basis of the primary starting material: (1) the Merck route via deoxycholine, (2) the Schering route and a subsequent manufacturing route via diosgenin, and (3) routes from phytosterols derived from soybeans.

3.2.1. Dexamethasone from Deoxycholic Acid. A patent filed by Merck in 1958[59] describes a slightly different route to dexamethasone than the publication,[57] introducing the C1−C2 double bond earlier than in the description provided in the journal article, and also provides a few more details. This route is presented herein.

The Merck route started with 3-α-acetoxy-16-pregnene-11,20-dione (**59**), a compound available from their manufacture of cortisone (Scheme 23) via deoxycholic acid (**58**). The conversion of deoxycholic acid to **59** was a major undertaking, requiring 16 steps.[60] Another eight steps afforded cortisone, while the synthesis of dexamethasone required an additional 17 steps, as described below.

The synthesis of dexamethasone from **59** began with the introduction of the 16-α-methyl group via conjugate addition using methylmagnesium iodide and cuprous bromide to afford **61** (Scheme 24). Several of the subsequent steps to intermediate **67** were adapted from those developed for the commercial

https://doi.org/10.1021/acs.oprd.1c00100
Org. Process Res. Dev. XXXX, XXX, XXX−XXX

manufacture of cortisone, as follows.[60] Introduction of the 17-α-hydroxy group involved the formation of a mixture of enol acetates **62**, epoxidation with perbenzoic acid to furnish **63**, and hydrolysis to reveal the hydroxy group and generate **64**. Installation of the C21 hydroxy group involved bromination followed by displacement with potassium acetate mediated by NaI to afford acetoxy product **65**. Oxidation of the C3 alcohol with chromium trioxide in pyridine afforded triketone **66**. Introduction of the C4−C5 double bond was accomplished by bromination at C4 followed by the formation of the bis(semicarbazide) at C3 and C20, resulting in dehydrobromination to generate **67**. The remaining ketone at C11 of bisprotected **67** was reduced with sodium borohydride, and then the bis(semicarbazide) was hydrolyzed with acid to provide **68**. Introduction of the C1−C2 double bond was carried out using an enzymatic dehydrogenase (*Bacillus sphaericus* (ATCC 245) or *Nocardia asteroides* (ATCC 9970)) to afford dienone **69** after acetylation of the C21 alcohol. The Merck publication introduced the double bond using SeO_2 either at this stage or as the final step, but no details of this transformation or yields were provided.[57b] Reaction with methanesulfonyl chloride provided triene **70**, which was treated with NaOBr, generated from *N*-bromosuccinimide (NBS) and aqueous perchloric acid, to form bromohydrin **71**, which in turn was ring-closed to give epoxide **72** by treatment with base. The final step, opening of the epoxide with HF to afford dexamethasone, was described in more detail.[59] Epoxide **72** was slurried in THF and cooled to −60 °C, and then HF/THF mixture (2:1 by weight) was added, and the resulting mixture was held at 5 °C for 2 h. After aqueous workup with potassium carbonate, the THF was removed by vacuum distillation to afford a slurry that was filtered and washed with chloroform to afford dexamethasone (**3**) with 94% purity (based on phase solubility measurements) in 70% yield. Further purification was accomplished by recrystallization from DMF/water.

3.2.2. Dexamethasone from Diosgenin. The Schering route described in the 1958 publication started with 16-α-methyldehydropregnenolone (**78**),[58a] a material that was derived from plant extracts by the Marker degradation (Scheme 25)[61] followed by introduction of the 16-α-methyl group using MeMgI.[62] This degradation process developed in the 1940s by Russell Marker opened the door for the production of several medicinal steroids. Marker went on to found Syntex, a company that was instrumental in introducing several commercial steroid drugs.

Scheme 25. Marker Degradation

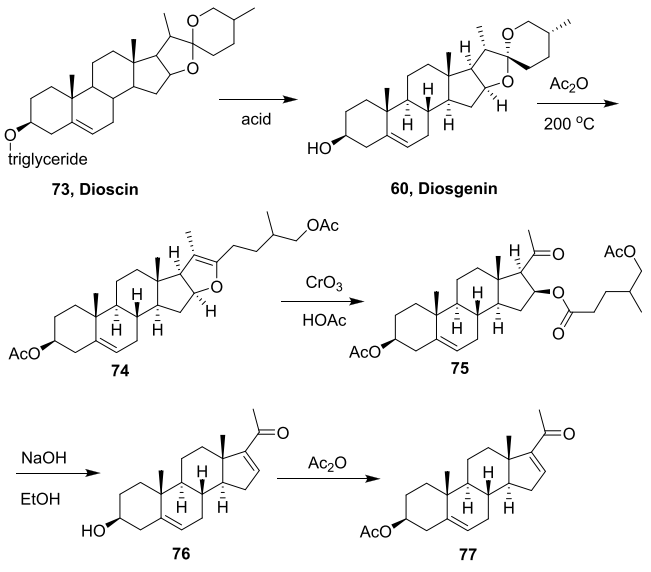

The starting material for the Schering route, **78**, differs from that used for the Merck route in that it does not have a ketone at the 11-position and it contains a C6−C7 double bond. A key transformation for this route was the microbial oxidation to install the hydroxy group at C11 position, a reaction initially discovered, developed, and published at Upjohn.[63] This discovery was a game-changer for the industrial production of cortisone and many follow-on steroids such as dexamethasone, allowing for use of plant sterols as starting materials instead of those derived from animal sources.

The Schering route began by hydrogenation of the C6−C7 double bond of **78** to provide **79** (Scheme 26).[58] The hydrogenation resulted in a trans ring junction of the A/B rings, which is different from the cis ring junction in the Merck route from **58**. This becomes an important factor for the introduction of the A-ring diene, as described below. The introduction of the 17-α-hydroxy group was carried out similarly to the Merck route via formation of the enol acetate, epoxidation, and ring opening to form **80**. Installation of the C21 acetoxy group and oxidation of the C3 hydroxy group was also carried out similarly to the Merck route, with bromination, displacement with acetate, and oxidation with chromium trioxide to form **81**. In the Merck process, bromination of **66** resulted in bromination only at the 4-position, leading to introduction of the C4−C5 double bond after dehydrobromination. With the trans A/B ring junction of **81**, bromination at both C2 and C4 was possible, generating **82**, which led to the introduction of both A-ring double bonds after dehydrobromination with DMF and NaOH to provide **83**. Installation of the C11 hydroxy group was accomplished via fungal fermentation with *Pestalotia foedans* to afford triol **84**. Schering later developed an alternate fungal strain, *Glomerella cingulate*, that was more productive for the 16-α-methyl compounds.[54b] Formation of the tosylate at the newly formed hydroxy position followed by elimination and reacylation at C21 provided **70**, at which point the synthesis intersected with the Merck route.

The discovery that the 11-hydroxy group could be installed in steroids via microbial fermentation allowed use of the plant steroid dioscin (**73**) as the source of starting material for the synthesis of many corticosteroids (Schering route). The longer route developed by Merck via the more expensive bovine bile acids was no longer an attractive approach. In the six decades since the first publication of the Schering route to dexamethasone, improvements to the route have been made using more modern chemistry[64] and a different order of steps. In a review of industrial syntheses of corticosteroids in 2017, Herraiz described a 14-step manufacturing route to dexamethasone from **77** (Scheme 27), available from **73** in four steps via Marker degradation (Scheme 25).[65]

While many of the steps in the second-generation route are similar to the original route, the ordering of the steps has changed. In the original Schering route (Scheme 26), the dihydroxyacetone fragment at C17 is installed first, while in the second-generation route (Scheme 27) this is installed at the end, thus requiring protection of the double bond of the enone as an epoxide. The second-generation synthesis started with epoxidation of **77** using basic hydrogen peroxide to provide epoxide **85** in which the acetate group has been hydrolyzed. Oppenauer

https://doi.org/10.1021/acs.oprd.1c00100
Org. Process Res. Dev. XXXX, XXX, XXX−XXX

Scheme 26. Schering Route to Dexamethasone

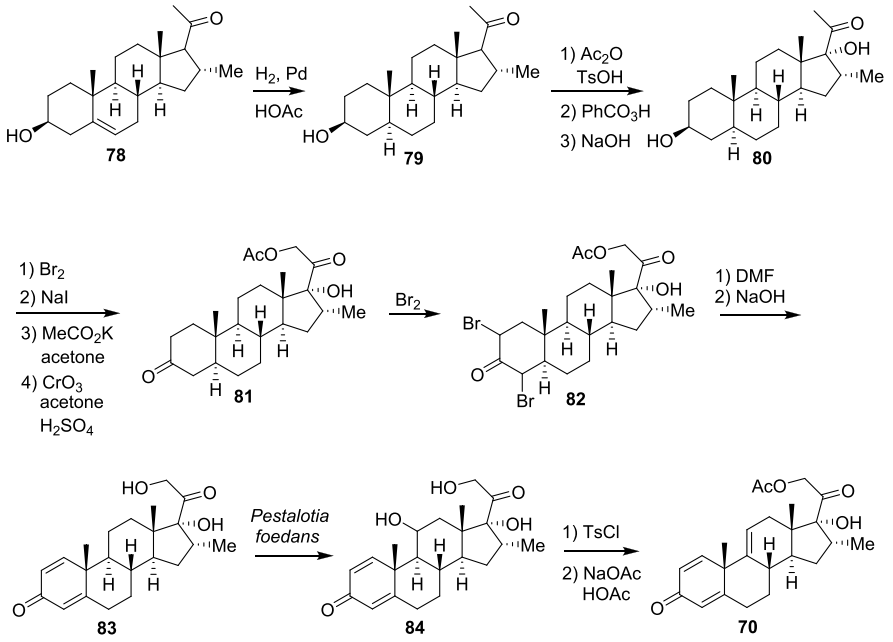

Scheme 27. Second Generation Route: A Manufacturing Synthesis of Dexamethasone

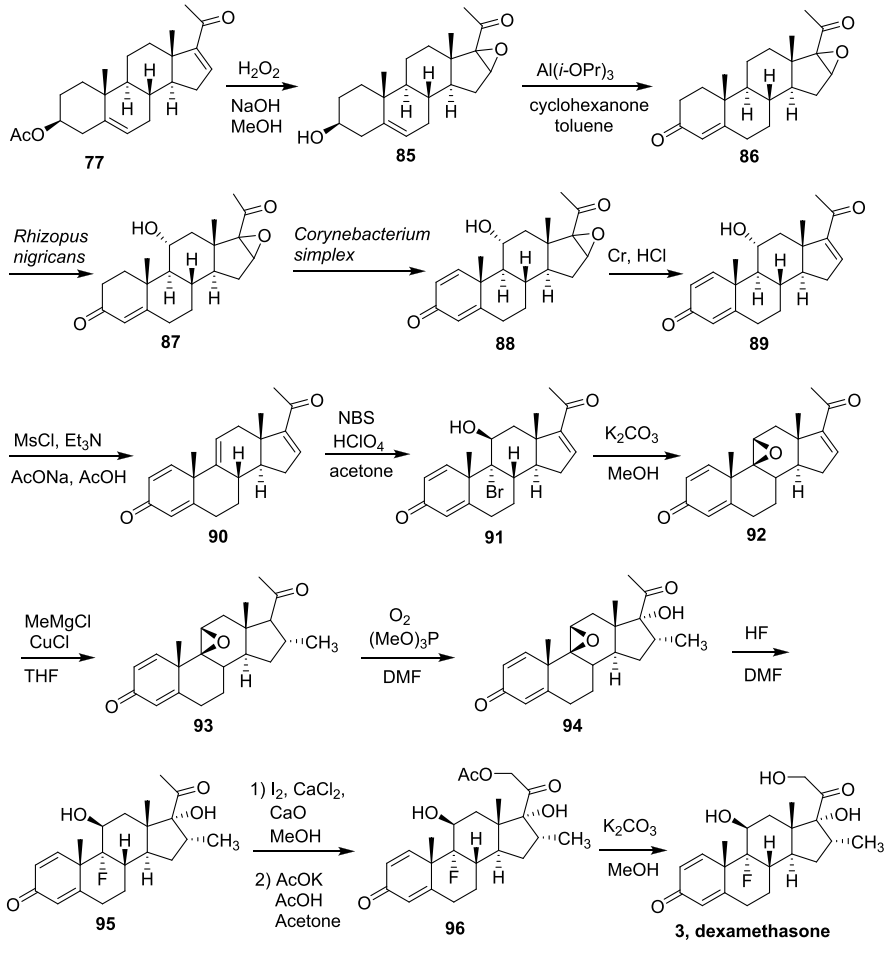

oxidation with aluminum isopropoxide to afford **86** not only oxidized the hydroxy group but also moved the C5−C6 double bond into the A ring, thereby avoiding the reduction−oxidation sequence in the original route, in which the double bond was hydrogenated and then reintroduced at a later time. This was followed by two biocatalytic oxidation steps, hydroxylation at the 11-position with the fungal strain *Rhizopus nigricans* to provide **87** followed by installation of the C1−C2 double bond

https://doi.org/10.1021/acs.oprd.1c00100
Org. Process Res. Dev. XXXX, XXX, XXX−XXX

Scheme 28. Route to Dexamethasone from Sitosterol

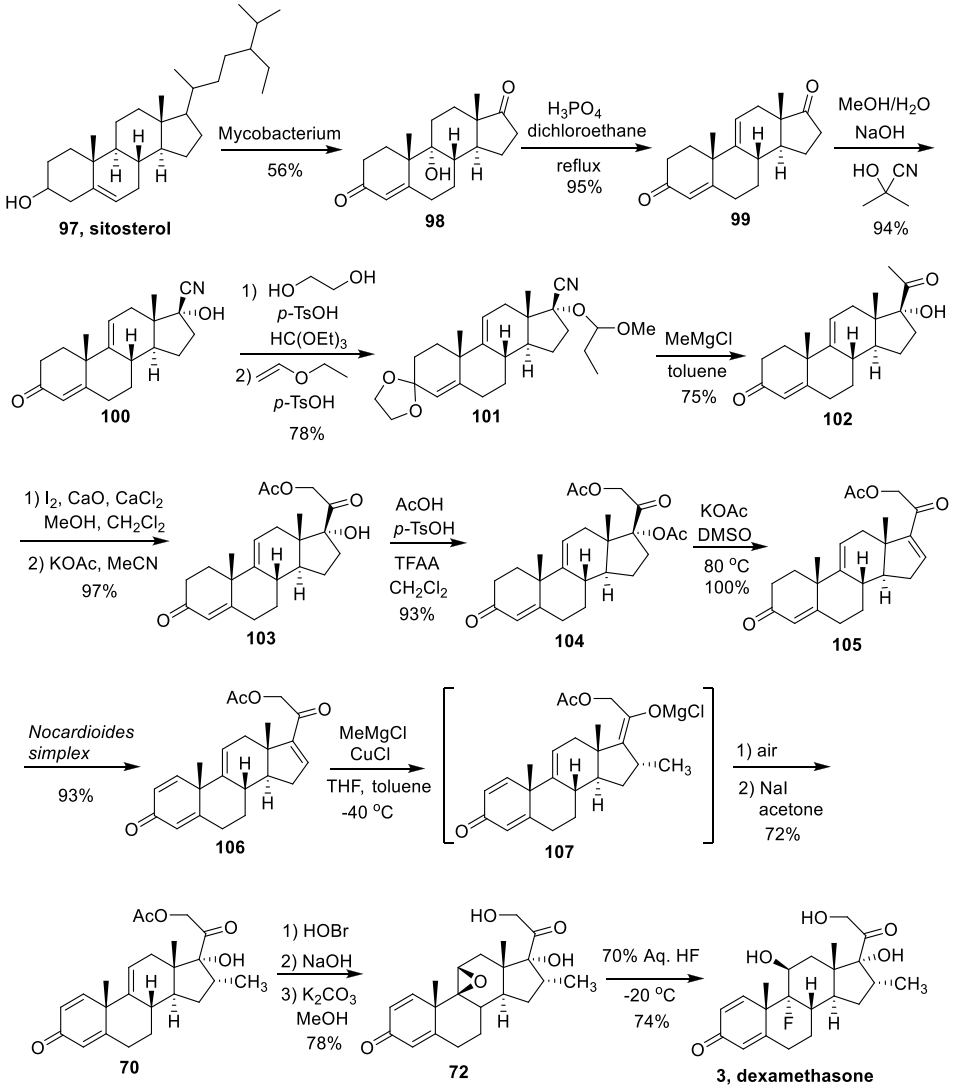

in **88** using *Corynebacterium simplex*. The discovery of the biocatalytic dehydrogenation was made serendipitously by Schering chemists in 1953 as they were attempting to find a biocatalytic method to hydrolyze the hindered acetate of the 11-position of dihydrocortisone 11,21-diacetate.[58b]

The C16−C17 double bond was reintroduced by reduction of the epoxide with chromium/HCl to furnish **89**. The C9−C11 double bond was then generated by mesylation of the C11 alcohol followed by elimination to afford tetraene **90**. Reaction with hypobromous acid, generated from aqueous perchloric acid and NBS in acetone, led to reaction only with the C9−C11 double bond to generate **91** since the other three double bonds are enones. Treatment with potassium carbonate in MeOH then afforded epoxide **92**. Introduction of the α-methyl group at C16 was carried out using MeMgCl with CuCl to afford **93**. The C17 hydroxy group was introduced using molecular oxygen and trimethyl phosphite in DMF, a procedure developed at Schering.[66] In the published procedure, the enolate anion was first generated in DMF from *t*-BuONa (prepared in situ from NaH and *t*-BuOH), after which trimethyl phosphite was added, the reaction mixture was cooled to −25 °C, oxygen was bubbled through the solution, and the substrate was added. The reaction first generates a hydroperoxide, which is reduced to the alcohol with trimethyl phosphite. The reaction was quenched with MeOH/water to afford **94**.[66] Given the safety concerns of operating with oxygen at manufacturing scale, this would be an excellent reaction to scale in flow, as was demonstrated by Bristol-Myers process chemists using this procedure on a different substrate.[67] The final steps involved opening of the epoxide with HF to furnish **95**. The C21 hydroxy group was then installed by iodination and displacement with acetate to provide **96** followed by basic hydrolysis to provide dexamethasone (**3**).

3.2.3. Routes to Dexamethasone via Phytosterols. While diosgenin (**60**), the key raw material for the preparation of dexamethasone and other medicinal steroids, is sourced from a renewable plant source, the process for its preparation via acid hydrolysis has created environmental concerns in China. In Hubei Province, China, about 1.5 million kg of diosgenin was produced annually in the early 2000s using hydrochloric acid or sulfuric acid to hydrolyze yellow ginger tubers.[68] With low pH, high sulfate content, and high chemical oxygen demand (COD), the wastewater created unmanageable pollution. Authorities shut down several producers, causing a reported 9-fold increase in the price of diosgenin from 2007 to 2015.[69]

With the availability of diogenin in question, routes from alternate plant sterols have been reconsidered. Phytosterols are

https://doi.org/10.1021/acs.oprd.1c00100
Org. Process Res. Dev. XXXX, XXX, XXX−XXX

byproducts of soybean oil production with wide abundance and low price. Upjohn and other companies developed a microbial fermentation process to convert sitosterol (**97**) and other phytosterols to androst-4-ene-3,17-dione and 9α-hydroxyandrost-4-ene-3,17-dione (**98**)[63a,70] and developed routes to several steroid drugs from these intermediates.[63a]

Described below is an 18-step route to dexamethasone from sitosterol, one of the phytosterols available from soybeans, that was disclosed in a 2014 Russian patent employing modifications of various steroid chemistries developed over the past 50 years (Scheme 28).[71] The route started with microbial cleavage of the hydrocarbon chain at C17 using *Mycobacterium* species to generate **98** in 56% yield after purification. It should also be noted that this process created the enone in the A ring and inserted the C9 hydroxy group. Treatment of **98** with phosphoric acid in refluxing dichloroethane resulted in the formation of the C9−C11 double bond of **99** in 95% yield. The two-carbon chain at C17 was constructed one carbon at a time. First, the nitrile was inserted using acetone cyanohydrin in basic MeOH/water using a procedure adapted from Nitta[72] to afford **100** in 94% yield. Protection of the C3 enone and the C17 hydroxy groups provided **101** in 78% yield. Addition of MeMgCl in toluene furnished **102** in 75% yield after hydrolysis of both protecting groups during workup. The C21 acetoxy group was inserted by α-iodination followed by displacement with acetate to form **103** in 97% yield. Use of iodine instead of bromine under these specified conditions reduced the amount of overhalogenation at C2 and C6. Conversion of the C17 hydroxy group to the C16−C17 double bond was accomplished by esterification at C17 as the acetate followed by treatment of the resulting **104** with KOAc in DMSO at 80 °C to afford **105** in quantitative yield.[73] Incorporation of the C1−C2 double bond by microbial fermentation afforded **106** in 93% yield. Introduction of the 16-α methyl group and C17 oxidation were carried out in a single pot. Methyl Grignard addition to **106** in toluene at −40 °C generated magnesium enolate **107**. This was exposed to air to produce the C17 hydroperoxide which was then reduced with NaI in acetone to afford **70** in 72% yield. Introduction of the C9 α-fluoro group followed the standard chemistry of epoxidation and ring opening with HF to furnish dexamethasone (**3**). This route appears to be viable for scale-up except for the C17 air oxidation step. An alternative oxidation of a similar compound using hydrogen peroxide could potentially be developed for this step to avoid use of air or oxygen (Scheme 29).[74]

Scheme 29. Alternate Oxidation at C17 using Hydrogen Peroxide

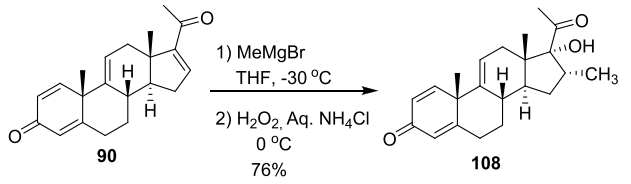

The introduction of the two-carbon chain at C17 one carbon at a time is also inefficient and requires protection and deprotection steps. A shorter three-step route from **99** to **105** was disclosed by Upjohn in 1980 in which the two-carbon fragment was added in a single step (Scheme 30).[75] This route started with protection of the A-ring enone of **99** as methyl enol ether **109**,[76] followed reaction of the C17 ketone with lithiated

Scheme 30. Upjohn Route to Dexamethasone via Two-Carbon Homologation

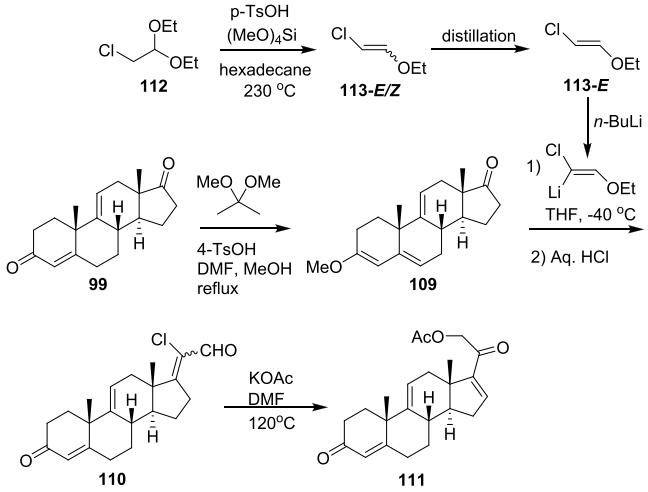

(*E*)-2-chloro-1-ethoxyethane (**113-*E***) to furnish aldehyde **110** as a mixture of geometric isomers in 91% isolated yield after workup with 6 N HCl. Treatment of **110** with KOAc in DMF at 120 °C afforded **105**, with no yield provided.

Much of this chemistry appears challenging to scale, such as the conversion of 2-chloroacetaldehyde dimethyl acetal (**112**) to 2-chloro-1-ethoxyethane (**113-*E*/*Z***) at 230 °C and the cryogenic temperature required for the 2-carbon homologation from **109** to **110**, but both reactions are prime candidates for the application of flow chemistry.

3.2.4. Summary of Routes to Dexamethasone. The discovery in the 1940s that cortisone could be a superb treatment for severely arthritic patients set off a highly competitive and innovative pursuit of steroidal analogues with an improved therapeutic index and pharmacokinetics. Dexamethasone emerged as one of the best drugs of those commercialized, with a reduced incidence of side effects and a longer half-life. The original route to dexamethasone developed by Schering-Plough in the 1950s from the plant source dioscin has held up well over the years. The current routes still use much of the chemistry developed by Schering-Plough and other pharmaceutical companies in the 1940s and 1950s. With the environmental issues created with the degradation process of dioscin in China, routes via phytosterols such as sitosterol, derived from soybeans, appear to be greener and more economically viable. With the amazing progress made in medicine over the past 60 years, it is remarkable that one of the effective treatments for COVID-19 comes from one of the oldest drugs in the medicine chest.

SUMMARY AND OUTLOOK

While progress toward a treatment of COVID-19 may seem painfully slow, in fact exceptional progress has been made within a year of the outbreak of the pandemic when viewed through the lens of the typical drug development timeline. Large-scale clinical trials have been conducted on dozens of repurposed small-molecule drugs. Of these, dexamethasone, remdesivir, and baricitinib (covered in our first article)[3] have emerged as partially effective therapies. On the basis of promising preclinical data, molnupiravir has an excellent chance to become a more efficacious treatment and as an oral treatment could find more widespread use outside the hospital setting. While not covered in

https://doi.org/10.1021/acs.oprd.1c00100
Org. Process Res. Dev. XXXX, XXX, XXX−XXX

this review of small molecules, three novel monoclonal antibodies have also been quickly developed to treat COVID-19.[77] Many new clinical candidates and repurposed drugs continue to be evaluated alone and in combination with other drugs in ongoing clinical trials. The development of SARS-CoV-2 vaccines has progressed at an unprecedented pace, with several vaccines now approved. With these vaccines now rolling out across the world, we can hope that disease prevention will minimize the need for disease treatments.

AUTHOR INFORMATION

Corresponding Author

David L. Hughes − *sp3 Pharma Consulting, San Diego, California 92121, United States;* orcid.org/0000-0001-5880-8529; Email: hughes.0987@gmail.com

Complete contact information is available at: https://pubs.acs.org/10.1021/acs.oprd.1c00100

Notes

The author declares no competing financial interest.

REFERENCES

(1) Ferreira, L. L. G.; Andricopulo, A. D. COVID-19: Small-Molecule Clinical Trials Landscape. *Curr. Top. Med. Chem.* **2020**, *20*, 1577−1580.

(2) (a) Ritchie, H.; Ortiz-Ospina, E.; Beltekian, D.; Mathieu, E.; Hasell, J.; Macdonald, B.; Giattino, C.; Appel, C; Roser, M. *How did confirmed deaths and cases change over time?* https://ourworldindata.org/mortality-risk-covid#how-did-confirmed-deaths-and-cases-change-over-time (accessed 2021-04-14). *The Case Fatality Rate (CFR) is the ratio between confirmed deaths and confirmed cases.* (b) D'Ambrosio, A. *Here's Why COVID-19 Mortality Has Dropped—There's No Single Answer, But a Host of Contributing Factors*. MedPage Today, November 17, 2020. https://www.medpagetoday.com/infectiousdisease/covid19/89750 (accessed 2021-04-14).

(3) De Savi, C.; Hughes, D. L.; Kvaerno, L. Quest for a COVID-19 Cure by Repurposing Small-Molecule Drugs: Mechanism of Action, Clinical Development, Synthesis at Scale, and Outlook for Supply. *Org. Process Res. Dev.* **2020**, *24*, 940−976.

(4) *FDA Approves First Treatment for COVID-19*. U.S. Food and Drug Administration, October 22, 2020. https://www.fda.gov/news-events/press-announcements/fda-approves-first-treatment-covid-19 (accessed 2021-04-14).

(5) *European Commission Grants Conditional Marketing Authorization for Gilead's Veklury® (remdesivir) for the Treatment of COVID-19*. Gilead Sciences, July 3, 2020. https://www.gilead.com/news-and-press/press-room/press-releases/2020/7/european-commission-grants-conditional-marketing-authorization-for-gileads-veklury-remdesivir-for-the-treatment-of-covid19 (accessed 2021-04-14).

(6) Beigel, J. H.; Tomashek, K. M.; Dodd, L. E.; Mehta, A. K.; Zingman, B. S.; Kalil, A. C.; Hohmann, E.; Chu, H. Y.; Luetkemeyer, A.; Kline, S.; et al. Remdesivir for the Treatment of Covid-19—Final Report. *N. Engl. J. Med.* **2020**, *383*, 1813−1826.

(7) WHO Solidarity Trial Consortium. Repurposed Antiviral Drugs for Covid-19—Interim WHO Solidarity Trial Results. *N. Engl. J. Med.* **2021**, *384*, 497−511.

(8) *WHO recommends against the use of remdesivir in COVID-19 patients*. World Health Organization, November 20, 2020. https://www.who.int/news-room/feature-stories/detail/who-recommends-against-the-use-of-remdesivir-in-covid-19-patients (accessed 2021-04-14).

(9) *Remdesivir*. IDSA, December 9, 2020. https://www.idsociety.org/covid-19-real-time-learning-network/therapeutics-and-interventions/remdesivir/ (accessed 2021-04-14).

(10) Spinner, C. D.; Gottlieb, R. L.; Criner, G. J.; Arribas Lopez, J. R.; Cattelan, A. M.; Soriano Viladomiu, A.; Ogbuagu, O.; Malhotra, P.; Mullane, K. M.; Castagna, A.; Chai, L. Y. A.; Roestenberg, M.; Tsang, O. T. Y.; Bernasconi, E.; Le Turnier, P.; Chang, S.-C.; SenGupta, D.; Hyland, R. H.; Osinusi, A. O.; Cao, H.; Blair, C.; Wang, H.; Gaggar, A.; Brainard, D. M.; McPhail, M. J.; Bhagani, S.; Ahn, M. Y.; Sanyal, A. J.; Huhn, G.; Marty, F. M. Effect of Remdesivir vs Standard Care on Clinical Status at 11 Days in Patients With Moderate COVID-19. A Randomized Clinical Trial. *JAMA* **2020**, *324*, 1048−1057.

(11) Lorenz, J. *Trial of Remdesivir for Moderate COVID-19 Shows Modest Results, Uncertainties*. Contagion Live, September 3, 2020. https://www.contagionlive.com/view/trial-of-remdesivir-for-moderate-covid19-shows-modest-results-uncertainties (accessed 2021-04-14).

(12) *Gilead Sciences Announces Fourth Quarter and Full Year 2020 Financial Results*. Gilead Sciences, February 4, 2021. http://investors.gilead.com/static-files/7227feec-53b9-4809-8181-fa1441f34f31 (accessed 2021-04-14).

(13) The routes to the triazine are summarized in the Supporting Information of the following article by the Sarpong and Garg groups: Knapp, R. R.; Tona, V.; Okada, T.; Sarpong, R.; Garg, N. K. Cyanoamidine Cyclization Approach to Remdesivir's Nucleobase. *Org. Lett.* **2020**, *22*, 8430−8435.

(14) Patil, S. A.; Otter, B. A.; Klein, R. S. Synthesis of Pyrrolo[2,1-*f*][1,2,4]triazine Congeners of Nucleic Acid Purines via the N-Amination of 2-Substituted Pyrroles. *J. Heterocycl. Chem.* **1994**, *31*, 781−786.

(15) Silverstein, R. M.; Ryskiewicz, E. E.; Willard, C. 2-Pyrrolealdehyde. *Org. Synth.* **1956**, *36*, 74.

(16) O'Connor, S. J.; Dumas, J.; Lee, W.; Dixon, J.; Cantin, D.; Gunn, D.; Burke, J.; Phillips, B.; Lowe, D.; Shelekhin, T.; Wang, G.; Ma, X.; Ying, S.; McClure, A.; Achebe, F.; Lobell, M.; Ehrgott, F.; Iwuagwu, C.; Parcella, K. Pyrrolo[2,1-*f*][1,2,4]triazin-4-ylamines Igf-1r Kinase Inhibitors for the Treatment of Cancer and other Hyperproliferative Diseases. WO 2007056170 A2. May 18, 2007.

(17) Loader, C. E.; Anderson, H. J. Pyrrole Chemistry. XXIII. The Cyanation of Substituted Pyrroles with Chlorosulfonyl Isocyanate (CSA). New Syntheses of Pyrrole-3-carbonitriles. *Can. J. Chem.* **1981**, *59*, 2673−2683.

(18) (a) Axt, S. D.; Badalov, P. R.; Brak, K.; Campagna, S.; Chtchemelinine, A.; Doerffler, E.; Frick, M. M.; Gao, D.; Heumann, L. V.; Hoang, B.; Lew, W.; Milburn, R. R.; Neville, S. T.; Ross, B.; Rueden, E.; Scott, R. W.; Siegel, D.; Stevens, A. C.; Tadeus, C.; Vieira, T.; Waltman, A. W.; Wang, X.; Whitcomb, M. C.; Wolfe, L.; Yu, C.-Y. Method for the Preparation of Ribosides. US 2020/0197422 A1, June 25, 2020. (b) Axt, S. D.; Badalov, P. R.; Brak, K.; Campagna, S.; Chtchemelinine, A.; Doerffler, E.; Frick, M. M.; Gao, D.; Heumann, L. V.; Hoang, B.; Lew, W.; Milburn, R. R.; Neville, S. T.; Ross, B.; Rueden, E.; Scott, R. W.; Siegel, D.; Stevens, A. C.; Tadeus, C.; Vieira, T.; Waltman, A. W.; Wang, X.; Whitcomb, M. C.; Wolfe, L.; Yu, C.-Y. Method for the Preparation of Ribosides. US 2016/0122356A, March 5, 2016.

(19) Zhang, Z.; Shen, M.; Zhao, L. Preparation Method of 7-Bromopyrrolo[2.1-*f*][1,2,4]-triazene-4-amine. CN 110845502, February 28, 2020.

(20) Juan, B. V.; Diez, J. A. A.; Albero, M. A. B.; Eastwood, P. R.; Trias, C. E.; Toribio, M. E. L.; Roberts, R. S.; Gispert, L. V.; Rodrigues, J. G.; Cepeda, M. M. New CRTh2 Antagonists. WO 2013010880 A1, January 24, 2013.

(21) Paymode, D. J.; Cardoso, F. S. P.; Agrawal, T.; Tomlin, J. W.; Cook, D. W.; Burns, J. M.; Stringham, R. W.; Sieber, J. D.; Gupton, B. F.; Snead, D. Expanding Access to Remdesivir via an Improved Pyrrolotriazine Synthesis: Supply Centered Synthesis. *Org. Lett.* **2020**, *22*, 7656−7661.

(22) (a) Clarke, M. O. H.; Jordan, R.; Mackman, R. L.; Ray, A.; Siegel, D. Methods for Treating Filoviridae Virus Infections. WO 2017/184668 A1, October 26, 2017. (b) Chun, B. K.; Clarke, M. O. H.; Doerffler, E.; Hul, H. C.; Jordan, R.; Mackman, R. L.; Parrish, J. P.; Ray, A. S.; Siegel, D. Methods for Treating Filoviridae Virus Infections. US 2019/0275063A1, September 12, 2019.

(23) Vieira, T.; Stevens, A.; Chtchemelinine, A.; Gao, D.; Badalov, P.; Heumann, L. Development of a Large-Scale Cyanation Process Using

Continuous Flow Chemistry en Route to the Synthesis of Remdesivir. *Org. Process Res. Dev.* **2020**, *24*, 2113−2121.
(24) Von Keutz, T.; Williams, J. D.; Kappe, C. O. Continuous Flow C-Glycosylation via Metal−Halogen Exchange: Process Understanding and Improvements toward Efficient Manufacturing of Remdesivir. *Org. Process Res. Dev.* **2020**, *24*, 2362−2368.
(25) Xue, F.; Zhou, X.; Zhou, R.; Zhou, X.; Xiao, D.; Gu, E.; Guo, X.; Xiang, J.; Wang, K.; Yang, L.; Zhong, W.; Qin, Y. Improvement of the C-glycosylation Step for the Synthesis of Remdesivir. *Org. Process Res. Dev.* **2020**, *24*, 1772−1777.
(26) (a) Imamoto, T.; Kusumoto, T.; Tawarayama, Y.; Sugiura, Y.; Mita, T.; Hatanaka, Y.; Yokoyama, M. Carbon-Carbon Bond-Forming Reactions using Cerium Metal or Organocerium(III) Reagents. *J. Org. Chem.* **1984**, *49*, 3904−3912. (b) Imamoto, T.; Takiyama, N.; Nakamura, K. Cerium Chloride-Promoted Nucleophilic Addition of Grignard Reagents to Ketones an Efficient Method for the Synthesis of Tertiary Alcohols. *Tetrahedron Lett.* **1985**, *26*, 4763−4766. (c) Imamoto, T.; Takiyama, N.; Nakamura, K.; Hatajima, T.; Kamiya, Y. Reactions of Carbonyl Compounds with Grignard Reagents in the Presence of Cerium Chloride. *J. Am. Chem. Soc.* **1989**, *111*, 4392−4398. (d) Sidler, D. R.; Sager, J. W.; Bergan, J. J.; Wells, K. M.; Bhupathy, M.; Volante, R. P. The Enantioselective Synthesis of LTD4 Antagonist L-708,738. *Tetrahedron: Asymmetry* **1997**, *8*, 161−168. (e) Liu, H.-J.; Shia, K.-S.; Shang, X.; Zhu, B.-Y. Organocerium Compounds in Synthesis. *Tetrahedron* **1999**, *55*, 3803−3830. (f) Conlon, D. A.; Kumke, D.; Moeder, C.; Hardiman, M.; Hutson, G.; Sailer, L. Insights into the Cerium Chloride-Catalyzed Grignard Addition to Esters. *Adv. Synth. Catal.* **2004**, *346*, 1307−1315. (g) Bartoli, G.; Cimarelli, C.; Marcantoni, E.; Palmieri, G.; Petrini, M. Highly Stereoselective Synthesis of α,β-Unsaturated Ketones by CeCl3Mediated Addition of Grignard Reagents to β-Enamino Ketones. *J. Chem. Soc., Chem. Commun.* **1994**, 715−716.
(27) Siegel, D.; Hui, H. C.; Doerffler, E.; Clarke, M. O.; Chun, K.; Zhang, L.; Neville, S.; Carra, E.; Lew, W.; Ross, B.; Wang, Q.; Wolfe, L.; Jordan, R.; Soloveva, V.; Knox, J.; Perry, J.; Perron, M.; Stray, K. M.; Barauskas, O.; Feng, J. Y.; Xu, Y.; Lee, G.; Rheingold, A. L.; Ray, A. S.; Bannister, R.; Strickley, R.; Swaminathan, S.; Lee, W. A.; Bavari, S.; Cihlar, T.; Lo, M. K.; Warren, T. K.; Mackman, R. L. Discovery and Synthesis of GS-5734, a Phosphoramidate Prodrug of a Pyrrolo[2,1-*f*][triazin-4-amino] Adenine *C*-Nucleoside for the Treatment of Ebola and Emerging Viruses. *J. Med. Chem.* **2017**, *60*, 1648−1661.
(28) Hu, T.; Xie, Y.; Liu, Y.; Xue, H.; Zhu, F.; Aisa, H. A.; Shen, J. A Convenient and Cost Efficient Route Suitable for "One-Pot" Synthesis of Molnupiravir. *ChemRxiv* **2021**, DOI: 10.26434/chemrxiv.14208206.v1.
(29) Wang, M.; Zhang, L.; Huo, X.; Zhang, Z.; Yuan, Q.; Li, P.; Chen, J.; Zou, Y.; Wu, Z.; Zhang, W. Catalytic Asymmetric Synthesis of the Anti-COVID-19 Drug Remdesivir. *Angew. Chem., Int. Ed.* **2020**, *59*, 20814−20819.
(30) Gannedi, V.; Villuri, B. K.; Reddy, S. N.; Ku, C.-C.; Wong, C.-H.; Hung, S.-C. Practical Remdesivir Synthesis through One-Pot Organocatalyzed Asymmetric (S)-P-Phosphoramidation. *J. Org. Chem.* **2021**, *86*, 4977−4985.
(31) Stuyver, L. J.; Whitaker, T.; McBrayer, T. R.; Hernandez-Santiago, B. I.; Lostia, S.; Tharnish, P. M.; Ramesh, M.; Chu, C. K.; Jordan, R.; Shi, J.; Rachakonda, S.; Watanabe, K. A.; Otto, M. J.; Schinazi, R. F. Ribonucleoside Analogue That Blocks Replication of Bovine Viral Diarrhea and Hepatitis C Viruses in Culture. *Antimicrob. Agents Chemother.* **2003**, *47*, 244−254.
(32) Sheahan, T. P.; Sims, A. C.; Zhou, S.; Graham, R. L.; Pruijssers, A. J.; Agostini, M. L.; Leist, S. R.; Schäfer, A.; Dinnon, K. H., III; Stevens, L. J.; Chappell, J. D.; Lu, X.; Hughes, T. M.; George, A. S.; Hill, C. S.; Montgomery, S. A.; Brown, A. J.; Bluemling, G. R.; Natchus, M. G.; Saindane, M.; Kolykhalov, A. A.; Painter, G.; Harcourt, J.; Tamin, A.; Thornburg, N. J.; Swanstrom, R.; Denison, M. R.; Baric, R. S. An Orally Bioavailable Broad-spectrum Antiviral Inhibits SARS-CoV-2 in Human Airway Epithelial Cell Cultures and Multiple Coronaviruses in Mice. *Sci. Transl. Med.* **2020**, *12*, eabb5883.
(33) Agostini, M. L.; Pruijssers, A. J.; Chappell, J. D.; Gribble, J.; Lu, X.; Andres, E. L.; Bluemling, G. R.; Lockwood, M. A.; Sheahan, T. P.; Sims, A. C.; Natchus, M. G.; Saindane, M.; Kolykhalov, A. A.; Painter, G. R.; Baric, R. S.; Denison, M. R. Small-Molecule Antiviral β-D-N^4-Hydroxycytidine Inhibits a Proofreading-Intact Coronavirus with a High Genetic Barrier to Resistance. *J. Virol.* **2019**, *93*, e01348-19.
(34) Urakova, N.; Kuznetsova, V.; Crossman, D. K.; Sokratian, A.; Guthrie, D. B.; Kolykhalov, A. A.; Lockwood, M. A.; Natchus, M. G.; Crowley, M. R.; Painter, G. R.; Frolova, E. I.; Frolov, I. β-D-N^4-Hydroxycytidine Is a Potent Anti-alphavirus Compound That Induces a High Level of Mutations in the Viral Genome. *J. Virol.* **2018**, *92*, e01965-17.
(35) Jena, N. R. Role of Different Tautomers on the Base-Pairing Abilities of Some of the Vital Antiviral Drugs used Against COVID-19. *Phys. Chem. Chem. Phys.* **2020**, *22*, 28115−28122.
(36) Cox, R. M.; Wolf, J. D.; Plemper, R. K. Therapeutically Administered Ribonucleoside Analogue MK-4482/EIDD-2801 Blocks SARS-CoV-2 Transmission in Ferrets. *Nature Microbiol.* **2021**, *6*, 11−18.
(37) *Merck and Ridgeback Bio Announce Closing of Collaboration and Licensing Transaction*. Merck, July 1, 2020. https://www.merck.com/news/merck-and-ridgeback-bio-announce-closing-of-collaboration-and-licensing-transaction/ (accessed 2021-04-14).
(38) *Efficacy and Safety of Molnupiravir (MK-4482) in Hospitalized Adult Participants with COVID-19 (MK-4482-001)*. https://clinicaltrials.gov/ct2/show/NCT04575584 (accessed 2021-04-14).
(39) *Ridgeback Biotherapeutics and Merck Announce Preliminary Findings from a Phase 2a Trial of Investigational COVID-19 Therapeutic Molnupiravir*. Merck, March 6, 2021. https://www.merck.com/news/ridgeback-biotherapeutics-and-merck-announce-preliminary-findings-from-a-phase-2a-trial-of-investigational-covid-19-therapeutic-molnupiravir/ (accessed 2021-04-14).
(40) Painter, G. R.; Bluemling, G. R.; Natchus, M. G.; Guthrie, D. N4-Hydroxycytidine and Derivatives and Anti-viral Uses Related Thereto. WO 2019113462, June 13, 2019.
(41) Steiner, A.; Znidar, D.; Ötvös, S. B.; Snead, D. R.; Dallinger, D.; Kappe, C. O. A High-Yielding Synthesis of EIDD-2801 from Uridine. Eur. *Eur. J. Org. Chem.* **2020**, *2020*, 6736−6739.
(42) Miah, A.; Reese, C. B.; Song, Q. Convenient Intermediates for the Preparation of C-4 Modified Derivatives of Pyrimidine Nucleosides. *Nucleosides Nucleotides* **1997**, *16*, 53−65.
(43) Gopalsamuthiram, V.; Williams, C.; Noble, J.; Jamison, T. F.; Gupton, B. F.; Snead, D. R. A Concise Route to MK-4482 (EIDD-2801) from Cytidine: Part 2. *Synlett* **2021**, *32*, 326−328.
(44) Vasudevan, N.; Ahlqvist, G. P.; McGeough, C. P.; Paymode, D. J.; Cardoso, F. S. P.; Lucas, T.; Dietz, J.-P.; Opatz, T.; Jamison, T. F.; Gupton, B. F.; Snead, D. *Chem. Commun.* **2020**, *56*, 13363−13364.
(45) Ahlqvist, G. P.; McGeough, C. P.; Senanayake, C.; Armstrong, J. D.; Yadaw, A.; Roy, S.; Ahmad, S.; Snead, D. R.; Jamison, T. F. Progress Towards a Large-Scale Synthesis of Molnupiravir (MK-4482, EIDD-2801) from Cytidine. *ChemRxiv* **2021**, DOI: 10.26434/chemrxiv.13809527.v1.
(46) Burke, A. J.; Birmingham, W. R.; Zhuo, Y.; Zucolota da Costa, B.; Crawshaw, R.; Thorpe, T. W.; Rowles, I.; Finnigan, J.; Charnock, S. J.; Lovelock, S. L.; Turner, N. J.; Green, A. P. A Biocatalytic Aapproach to a Key Intermediate for the Synthesis of the COVID-19 Experimental Drug Molnupiravir. *ChemRxiv* **2021**, DOI: 10.26434/chemrxiv.13721692.v1.
(47) Benkovics, T.; McIntosh, J. A.; Silverman, S. M.; Kong, J.; Maligres, P.; Itoh, T.; Yang, H.; Huffman, M. A.; Verma, D.; Pan, W.; Ho, H.-I.; Vroom, J.; Knight, A.; Hurtak, J.; Morris, W.; Strotman, N. A.; Murphy, G.; Maloney, K. M.; Fier, P. S. Evolving to an Ideal Synthesis of Molnupiravir, an Investigational Treatment for COVID-19. *ChemRxiv* **2020**, DOI: 10.26434/chemrxiv.13472373.v1.
(48) Ahmed, M. H.; Hassan, A. Dexamethasone for the Treatment of Coronavirus Disease (COVID-19): a Review. *SN Compr. Clin. Med.* **2020**, *2*, 2637−2646.
(49) Horby, P.; Lim, W. S.; Emberson, J. R.; Mafham, M.; Bell, J. L.; Linsell, L.; Staplin, N.; Brightling, C.; Ustianowski, A.; Elmahi, E.;

Prudon, B.; Green, C.; Felton, T.; Chadwick, D.; Rege, K.; Fegan, C.; Chappell, L. C.; Faust, S. N.; Jaki, T.; Jeffery, K.; Montgomery, A.; Rowan, K.; Juszczak, E.; Baillie, J. K.; Haynes, R.; Landray, M. J. Dexamethasone in Hospitalized Patients with Covid-19 - Preliminary Report. *N. Engl. J. Med.* **2021**, *384*, 693−704.

(50) Tomazini, B.; Maia, I. S.; Cavalcanti, A. B.; Berwanger, O.; Rosa, R. G.; Veiga, V. C.; Avezum, A.; Lopes, R. D.; Bueno, F. R.; Silva, M. V. A. O.; Baldassare, F. P.; Costa, E. L. V.; Moura, R. A. B.; Honorato, M. O.; Costa, A. N.; Damiani, L. P.; Lisboa, T.; Kawano-Dourado, L.; Zampieri, R. G.; Olivato, G. B.; Righy, C.; Amendola, C. P.; Roepke, R. M. L.; Freitas, D. H. M.; Forte, D. N.; Freitas, F. G. R.; Fernandes, C. C. F.; Melro, L. M. G.; Junior, G. F. S.; Morais, D. C.; Zung, S.; Machado, F. R.; Azevedo, L. C. P Effect of Dexamethasone on Days Alive and Ventilator-Free in Patients with Moderate or Severe Acute Respiratory Distress Syndrome and COVID-19: The CoDEX Randomized Clinical Trial. *JAMA* **2020**, *324*, 1307−1316.

(51) Jie Jack Li has authored a recent on-line review of the history of dexamethasone. See: Li, J. J. *The Story of Dexamethasone*. https://www.chempartner.com/2020/07/01/the-story-of-dexamethasone/ (accessed 2021-04-14).

(52) Sarett, L. H. Partial Synthesis of Pregnene-4-triol-17β,20β,21-dione-3,11 and Pregnene-4-diol-17β,21-trione-3,11,20 Monoacetate. *J. Biol. Chem.* **1946**, *162*, 601−631.

(53) Hirschmann, R. The Cortisone Era: Aspects of its Impact. Some Contributions of the Merck Laboratories. *Steroids* **1992**, *57*, 579−592.

(54) (a) *History of cortisone's discovery offers lessons in 'team science,' persistence*. Healio, April 3, 2017. https://www.healio.com/news/endocrinology/20170403/history-of-cortisones-discovery-offers-lessons-in-team-science-persistence (accessed 2021-04-14). (b) Glyn, J. H. The Discovery of Cortisone: A Personal Memory. *Br. Med. J.* **1998**, *317*, 822. (c) Burns, C. M. The History of Cortisone Discovery and Development. *Rheumatic Disease Clinics of North America* **2016**, *42*, 1−14.

(55) McKay, L. I.; Cidlowski, J. A. Pharmacokinetics of Corticosteroids. In *Holland-Frei Cancer Medicine*, 6th ed.; Kufe, D. W., Pollock, R. E., Weichselbaum, R. R., Eds.; Decker: Hamilton, Ontario, 2003; https://www.ncbi.nlm.nih.gov/books/NBK13300/ (accessed 2021-04-14).

(56) Fried, J.; Sabo, E. F. Synthesis of 17α-Hydroxycorticosterone and its 9α-Halo Derivatives from 11-Epi-17α-hydroxycorticosterone. J. Am. Chem. Soc. 1953, 75, 2273−2274. (b) Fried, J.; Sabo, E. F. 9α-Fluoro Derivatives of Cortisone and Hydrocortisone. *J. Am. Chem. Soc.* **1954**, *76*, 1455−1456.

(57) (a) Arth, G. E.; Johnston, D. B. R.; Fried, J.; Spooncer, W. W.; Hoff, D. R.; Sarett, L. H. 16-Methylated Steroids. I. 16α-Methylated Analogs of Cortisone, A New Group of Anti-Inflammatory Steroids. *J. Am. Chem. Soc.* **1958**, *80*, 3160−3161. (b) Arth, G. E.; Fried, J.; Johnston, D. B. R.; Hoff, D. R.; Sarett, H. L.; Silber, R. H.; Stoerk, H. C.; Winter, C. A. 16-Methylated Steroids. II. 16α-Methyl Analogs of Cortisone, a New Group of Anti-Inflammatory Steroids. 9α-Halo Derivatives. *J. Am. Chem. Soc.* **1958**, *80*, 3161−3163.

(58) (a) Oliveto, E. P.; Rausser, R.; Weber, L.; Nussbaum, A. L.; Gebert, W.; Coniglio, C. T.; Hershberg, E. B.; Tolksdorf, S.; Eisler, M.; Perlman, P. L.; Pechet, M. M. 16-Alkylated Corticoids. II. 9α-Fluoro-16α-MethylPrednisolone 21-Acetate. *J. Am. Chem. Soc.* **1958**, *80*, 4431. For a review of the steroid program at Schering, see: (b) Herzog, H.; Oliveto, E. P. A History of Significant Steroid Discoveries and Developments Originating at the Schering Corporation (USA) Since 1948. *Steroids* **1992**, *57*, 617−623.

(59) Hirshmann, R. F. Improved Process for the Production of Fluoro Hydroxy Steroids. US 3,049,556, August 14, 1962.

(60) Pines, S. H. The Merck Bile Acid Cortisone Process: The Next-to-Last Word. *Org. Process Res. Dev.* **2004**, *8*, 708−724.

(61) Marker, R. E.; Tsukamoto, T.; Turner, D. L. Sterols. C. Diosgenin. *J. Am. Chem. Soc.* **1940**, *62*, 2525−2532.

(62) Marker, R. E.; Crooks, H. M. Sterols. CXLIV. Some 16-Alkylpregnenolones and Progesterones. *J. Am. Chem. Soc.* **1942**, *64*, 1280−1281.

(63) (a) Hogg, J. A. Steroids, the Steroid Community, and Upjohn in Perspective: a Profile of Innovation. *Steroids* **1992**, *57*, 593−616. For a review of the steroid development program at Upjohn, see: (b) Peterson, D. H.; Murray, H. C. Microbiological Oxygenation of Steroids at Carbon-11. *J. Am. Chem. Soc.* **1952**, *74*, 1871−1872. (c) Peterson, D. H.; Murray, H. C.; Eppstein, S. H.; Reineke, L. M.; Weintraub, A.; Meister, P. D.; Leigh, H. M. Microbiological Transformation of Steroids. I. Introduction of Oxygen at Carbon11 of Progesterone. *J. Am. Chem. Soc.* **1952**, *74*, 5933−5936. (d) Meister, P. D.; Peterson, D. H.; Murray, H. C.; Eppstein, S. H.; Reineke, L. M.; Weintraub, A.; Leigh, H. M. Microbiological Transformations of Steroids. II. The Preparation of 11α-Hydroxy-17α-progesterone. *J. Am. Chem. Soc.* **1953**, *75*, 55−57. (e) Peterson, D. H.; Murray, H. C. Oxygenation of Steroids by Mucorales Fungi. US 2602769, July 8, 1952.

(64) Ohta, T.; Zhang, H.; Torihara, Y.; Furukawa, I. Improved Synthetic Route to Dexamethasone Acetate from Tigogenin. *Org. Process Res. Dev.* **1997**, *1*, 420−424.

(65) Herráiz, I. Chemical Pathways of Corticosteroids, Industrial Synthesis from Sapogenins. *Methods Mol. Biol.* **2017**, *1645*, 15−27.

(66) Gardner, J. N.; Carlon, F. E.; Gnoj, O. OneSstep Procedure for the Preparation of Tertiary Alpha-Ketols from the Corresponding Ketones. *J. Org. Chem.* **1968**, *33*, 3294−3297.

(67) LaPorte, T. L.; Hamedi, M.; DePue, J. S.; Shen, L.; Watson, D.; Hsieh, D. Development and Scale-Up of Three Consecutive Continuous Reactions for Production of 6-Hydroxybuspirone. *Org. Process Res. Dev.* **2008**, *12*, 956−966.

(68) Liu, W.; Huang, W.; Sun, W.; Zhu, Y.; Ni, J. Production of Diosgenin from Yellow Ginger (Dioscorea zingiberensis C. H. Wright) Saponins by Commercial Cellulase. *World J. Microbiol. Biotechnol.* **2010**, *26*, 1171−1180.

(69) Qiu, W.; Jiang, C.; Gu, X.; Lin, L. Preparation Method of Dexamethasone Intermediate. CN 105440094, March 30, 2016.

(70) (a) Wovcha, M. G.; Antosz, F. J.; Knight, J. C.; Kominek, L. A.; Pyke, T. R. Bioconversion of Sitosterol to Usefu1 Steroidal Intermediates by Mutants of Mycobacterium Fortuitum. *Biochim. Biophys. Acta, Lipids Lipid Metab.* **1978**, *531*, 308−321. (b) Wovcha, M. G.; Biggs, C. B. Process for Preparing Androst-4-ene-3,17-dione. US 4,293,644, October 6, 1981. (c) Sih, C. J.; Weisenborn, F. L. Process for Preparing 9-α-Hydroxy Steroids. US 3,065,146, November 20, 1962.

(71) Vitalievich, K. A.; Stepanovna, S. T.; Vadimovich, L. N.; Vladimirovich, D. D.; Makhailovich, K. S.; Viktorovna, S. G.; Anatolievich, S. A.; Valerievna, F. V.; Maximovna, N. V.; Viktorovna, D. M.; Valerievna, E. O.; Vasilievich, S. V. Method of Obtaining 11β,17α,21-Trihydroxy-16α-methyl-9α-fluoropregna-1,4-diene-3,20-dione (Dexamethasone) from Phytosterol. RU 0002532902, November 20, 2014.

(72) Nitta, I.; Fujimori, S.; Ueno, H. The Syntheses of the Corticoid Side Chain. I. An Improved Method for Preparation of 17α-Hydroxyprogesterone from Androst-4-ene-3,17-dione. *Bull. Chem. Soc. Jpn.* **1985**, *58*, 978−980.

(73) (a) Salce, L.; Hazen, G. G.; Schoenewaldt, E. F. Preparation of 16-Unsaturated Steroids by Elimination of 17Alpha-Acyloxyl. *J. Org. Chem.* **1970**, *35*, 1681−1682. (b) Solo, A. J.; Suto, M. J. Effects of C-21 Substituents on the Elimination from 17-alpha-(Acyloxy)-20-Oxosteroids. *J. Org. Chem.* **1980**, *45*, 2012−2013.

(74) Wang, F.; Zhou, J.; Jiang, J.; Li, J. Method for Preparing Dexamethasone and Series Products Thereof. CN 1397320, April 1, 2009.

(75) Hessler, E. J.; Van Rheenen, V. H. Synthesis of 16-Unsaturated Pregnanes from 17-Ketosteroids. US 4,216,159, August 5, 1980.

(76) Nussbaum, A. L.; Yuan, E.; Dincer, D.; Oliveto, E. P. Enol Ethers of Steroidal Δ4−3-Ketones. *J. Org. Chem.* **1961**, *26*, 3925−3928.

(77) For a summary of treatment options, see: *Treatments for COVID-19*. Harvard Medical School, April 5, 2021. https://www.health.harvard.edu/diseases-and-conditions/treatments-for-covid-19 (accessed 2021-04-14).

https://doi.org/10.1021/acs.oprd.1c00100
Org. Process Res. Dev. XXXX, XXX, XXX−XXX